

Bertalan Juhasz *et al.*

Supporting Information

Dermacozine N, the First Natural Linear Pentacyclic Oxazinophenazine with UV-Vis Absorption Maxima in the Near Infrared Region, along with Dermacozines O and P Isolated from the Mariana Trench Sediment Strain *Dermacoccus abyssi* MT 1.1^T

Bertalan Juhasz ¹, Dawrin Pech-Puch ², Jioji N. Tabudravu ³, Bastien Cautain ⁴, Fernando Reyes ⁴, Carlos Jiménez ⁵, Kwaku Kyeremeh ⁶ and Marcel Jaspars ^{1*}

¹ Marine Biodiscovery Centre, Department of Chemistry, University of Aberdeen, Old Aberdeen, Scotland, AB24 3UE, UK; r01bj16@abdn.ac.uk

² Departamento de Biología Marina, Universidad Autónoma de Yucatán, Km. 15.5, carretera Mérida-Xmatkuil, A.P. 4-116 Itzimná, C.P. 97100 Mérida, Yucatán, México; dawrin.j.pech@udc.es

³ School of Natural Sciences, Faculty of Science and Technology, University of Central Lancashire, Preston, PR1 2HE, UK; JTabudravu@uclan.ac.uk

⁴ Fundación MEDINA, Centro de Excelencia en Investigación de Medicamentos Innovadores en Andalucía Avda. del Conocimiento 34, Edificio Centro de Desarrollo Farmacéutico y Alimentario, Parque Tecnológico de Ciencias de la Salud 18016 Granada, Spain; cautainbastien@gmail.com (B.C.); fernando.reyes@medinaandalucia.es (F.R.)

⁵ Centro de Investigaciónes Científicas Avanzadas (CICA) e Departamento de Química, Facultade de Ciencias, AE CICA-INIBIC, Universidad da Coruña, 15071 A Coruña, Spain; carlos.jimenez@udc.es

⁶ Marine and Plant Research Laboratory of Ghana, Department of Chemistry, School of Physical and Mathematical Sciences, University of Ghana, P.O. Box LG 56, Legon-Accra, Ghana; kkyeremeh@ug.edu.gh

* Correspondence: m.jaspars@abdn.ac.uk, Tel.: +44-1224-272-895

Bertalan Juhasz et al.

Contents

Figure S1. LC-MS analysis of dermacozine N (1) (qTOF, Bruker).....	6
Figure S2. MS/MS of dermacozine N (1) (qTOF, Bruker)	6
Figure S3A. Proposed MS fragmentation pathway of dermacozine N (1) showing loss of a (-ON(C ₆ H ₄)-) fragment.	7
Figure S3B. Mass Error between the calculated (Chemdraw modelled) and experimental (qTOF) <i>m/z</i> ratio of dermacozine N (1)	7
Figure S4. UV-Vis spectrum of dermacozine N (1) in EtOH.....	8
Figure S6. Dermacozine N (1) ¹ H-NMR spectrum (800 MHz, DMSO- <i>d</i> ₆).....	9
Figure S7. ¹ H- ¹³ C HSQC spectrum of dermacozine N (1) (800 MHz, DMSO- <i>d</i> ₆).....	9
Figure S8. ¹ H- ¹³ C HMBC (magnitude mode) spectrum of dermacozine N (1) (800 MHz, DMSO- <i>d</i> ₆) Inlets show the H-2 to C-11 carbonyl correlation (top left, phase sensitive mode), the <i>ortho</i> -substituted D-ring (top right, magnitude mode) and N-methyl C4a, C5a correlation (bottom right, phase sensitive mode)	10
Figure S9. ¹ H- ¹³ C HMBC spectrum of dermacozine N (1) with 2 Hz Coupling (800 MHz, DMSO- <i>d</i> ₆).....	10
Figure S10. ¹ H- ¹ H COSY spectrum of dermacozine N (1) (800 MHz, DMSO- <i>d</i> ₆)	11
Figure S11. ¹ H- ¹ H NOESY spectrum of dermacozine N (1) (800 MHz, DMSO- <i>d</i> ₆) (Inlets show the N-methyl and H-4 (top), and NH ₂ -12 to H-9 (middle and lower) correlations)	12
Figure S12. ¹ H- ¹⁵ N HMBC spectrum of dermacozine N (1) (800 MHz, DMSO- <i>d</i> ₆)	13
Figure S13. LC-MS analysis of dermacozine O (2) (qTOF, Bruker).....	13
Figure S14. UV-Vis spectrum of dermacozine O (2) in EtOH	14
Figure S15. IR spectrum of dermacozine O (2) in EtOH.....	14
Figure S16. ¹ H-NMR spectrum of dermacozine O (2) (800 MHz, DMSO- <i>d</i> ₆).....	15
Figure S17. ¹ H- ¹³ C HSQC spectrum of dermacozine O (2) (800 MHz, DMSO- <i>d</i> ₆)	15
Figure S18. ¹ H- ¹³ C HMBC spectrum of dermacozine O (2) (800 MHz, DMSO- <i>d</i> ₆) (Inlets show NH-14 and C-6, C-16 correlations (top), N-methyl hydrogen atom to C4a and C5a correlations (middle), H2 to C-11 carbonyl correlation (bottom))	16
Figure S19. Long Range ¹ H- ¹³ C HMBC correlations of Dermacozine O (2) with <i>J</i> = 2Hz (800 MHz, DMSO- <i>d</i> ₆)	16
Figure S20. ¹ H- ¹ H COSY spectrum of dermacozine O (2) (800 MHz, DMSO- <i>d</i> ₆)	17

Bertalan Juhasz et al.

Figure S21. ^1H - ^{15}N HMBC spectrum of dermacozine O (2) (800 MHz, DMSO- d_6).....	17
Figure S22. UV-Vis spectrum of dermacozine P (3) in EtOH.....	18
Figure S23. IR spectrum of dermacozine P (3) in EtOH.....	18
Figure S24. LC-MS analysis of dermacozine P (3) (Orbitrap, Xcalibur)	19
Figure S25. MS/MS analysis of dermacozine P (3) (Orbitrap, Xcalibur)	19
Figure S26. ^1H -NMR spectrum of dermacozine P (3) (600 MHz, DMSO- d_6).....	20
Figure S27. ^1H - ^{13}C HSQC spectrum of dermacozine P (3) (600 MHz, DMSO- d_6).....	20
Figure S28. ^1H - ^{13}C HMBC spectrum of dermacozine P (3) (600 MHz, DMSO- d_6).....	21
Figure S29. ^1H - ^1H COSY spectrum of dermacozine P (3) (600 MHz, DMSO- d_6)	21
Figure S30. 1D-NOESY spectrum of dermacozine P (3) (600 MHz, DMSO- d_6) from irradiation of the signal at 8.03 ppm.....	22
Figure S31. ^{13}C -NMR δ calculated values of dermacozine A-D (4-7) using the ACD Labs software with Neural Network Algorhitm Algorithm, solvent DMSO- d_6	22
Figure S32. ^{13}C -NMR δ calculated values of dermacozine E-H (8-11) using the ACD Labs Software with Neural Network Algorhitm Algorithm, solvent DMSO- d_6	23
Figure S33. ^{13}C -NMR δ calculated values of dermacozine I-J (12-13) and dermacozine M-P (14, 1-3) using the ACD Labs Software with Neural Network Algorhitm Algorithm, solvent DMSO- d_6	23
Figure S34. ^{13}C -NMR δ calculated values of possible structures (A-F) of dermacozine N (1), using the ACD Labs Software with Neural Network Algorhitm Algorithm, solvent DMSO- d_6	24
Figure S35. ^{13}C -NMR δ calculated values of possible structures (G-L) of dermacozine N (1), using the ACD Labs Software with Neural Network Algorhitm Algorithm, solvent DMSO- d_6	24
Figure S36. ^{13}C -NMR δ calculated values of possible structures (M-R) of dermacozine N (1), using the ACD Labs Software with Neural Network Algorhitm Algorithm, solvent DMSO- d_6	25
Figure S37. ^{13}C -NMR δ calculated values of possible structures (S-U) of dermacozine N (1), using the ACD Labs Software with Neural Network Algorhitm Algorithm, solvent DMSO- d_6	25
Figure S38. ^{13}C -NMR δ calculated values of possible structures (V and W) of dermacozine N (1), using the ACD Labs Software with Neural Network Algorhitm Algorithm, solvent DMSO- d_6	26
Table S1. Comparison between calculated vs. experimental ^{13}C -NMR δ values of dermacozines A-J (4-13)	27
Figure 39. Linear regression graphics between ACD Labs (Neural Network Algorithm) calculated vs. experimental ^{13}C -NMR δ values of dermacozine A-H (4-11).....	28

Bertalan Juhasz et al.

Table S2. Comparison between the experimental ^{13}C -NMR δ values of dermacozine N (1) vs. the calculated ones of possible structures A , D , E , G , H , I , J , K , N , P , Q , V , W by ACD Labs (Neural Network Algorithm, DMSO- d_6)	30
Figure S41. Linear regression graphics between ^{13}C -NMR δ experimental values of dermacozine N (1) vs. the ACD Labs calculated ones (Neural Network Algorithm, DMSO- d_6) (4-13).....	31
Figure S42. Linear regression graphics between ^{13}C -NMR δ experimental values of dermacozine N (1) vs. the ACD Labs (Neural Network Algorithm, DMSO- d_6) calculated ones for possible structures N , P , Q , V , W	32
Table S3. Absolute Error and the standard deviation of the error from the mean between the calculated (Structure W) and the experimental dermacozine N (1) ^{13}C -NMR chemical shifts	33
Table S4. Experimental values of ^{13}C -NMR δ chemical shifts of dermacozines E (8), F (9), G (9) and O (2) for multiple regression and t-test	34
Figure S43. Multiple regression analysis between the experimental ^{13}C -NMR δ values of dermacozines E (8), F (9), G (9) as independent variables and those of dermacozine O (2) as dependent variables	37
Table S5. Residuals between the observed and predicted values of ^{13}C -NMR δ of dermacozines E (8), F (9), G (9) as independent variables and those of dermacozine O (2) as dependent variables	38
Table S6. Comparison between experimental and the ACD Labs calculated ^{13}C -NMR δ chemical shift values of dermacozines P (3) (Neural Network Algorithm, DMSO- d_6)....	39
Figure S44. Linear regression graphics between the experimental ^{13}C -NMR δ chemical shifts of dermacozine P (3) and the ACD Labs calculated ^{13}C -NMR δ values (Neural Network Algorithm, DMSO- d_6)	40
Table S7. Absolute Error and the standard deviation of the error from the mean between the calculated and the experimental dermacozine P (3) ^{13}C -NMR chemical shifts	41
Figure S45. Evaluation of the cytotoxic activity of dermacozine N (1) against human A) Melanoma (A2058) and B) Hepatocellular carcinoma (HepG2) cell lines (IC ₅₀ graphs) ..	42
Table S8. Experimental NMR spectroscopic data for dermacozine N (1) with HMBC, COSY and NOESY correlations (800 MHz, DMSO- d_6)	43
Table S9. Experimental NMR spectroscopic data for dermacozine O (2) with HMBC and COSY correlations (800 MHz, DMSO- d_6).....	44
Table S10. Experimental NMR spectroscopic data for dermacozine P (3) with HMBC and COSY correlations (600 MHz, DMSO- d_6).....	45
Figure S46. Workflow of dermacozine N (1) structure determination	46

Bertalan Juhasz et al.

Figure S47. Workflow of dermacozine O (2) structure determination	47
Figure S48. Workflow of dermacozine P (3) structure determination	48
Theme S1. Dermacozine N (1) H-9 and NH ₂ -12 distance (Modelled with Chemdraw, Chem 3D).....	49
Theme S2. TLC plate of the initial FD fraction following Kupchan liquid-liquid partitioning, showing the colorful bands where the dermacozines were isolated from (left) and the same TLC plate under UV 360 nm light (right).....	50
Theme S3. HPLC chromatogram for the isolation of dermacozine O (2).....	50
Theme S4. HPLC chromatogram for the isolation of dermacozine P (3)	51

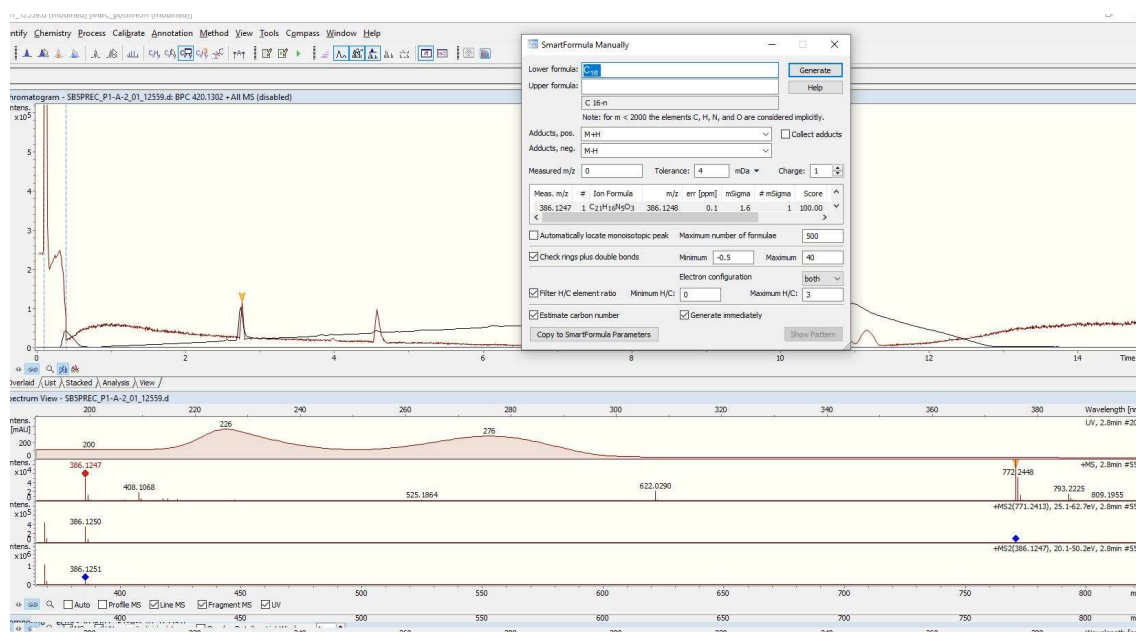


Figure S1. LC-MS analysis of dermacozine N (1) (qTOF, Bruker)

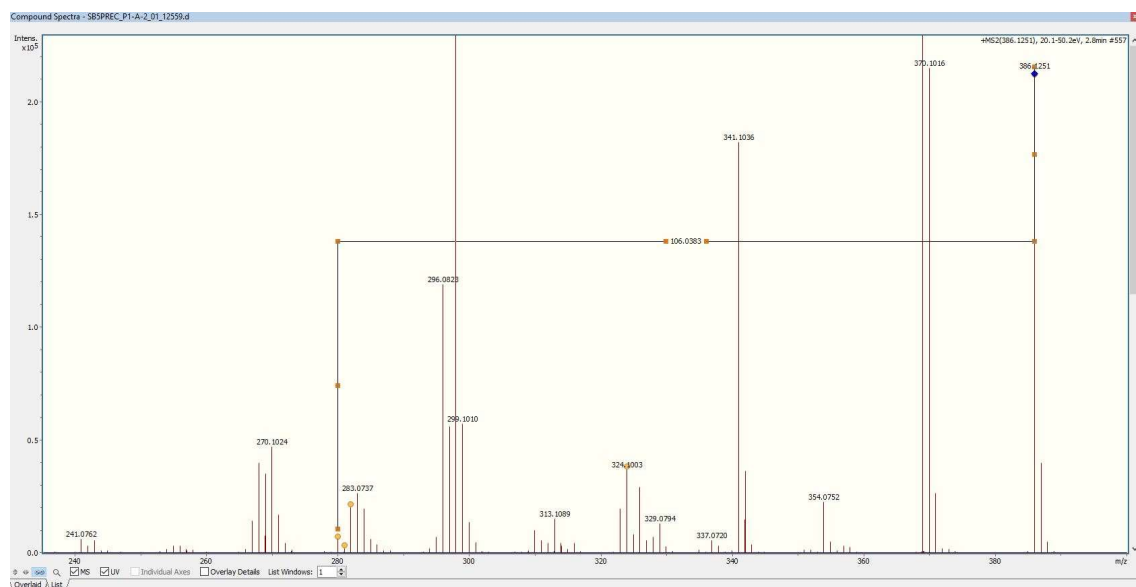


Figure S2. MS/MS of dermacozine N (1) (qTOF, Bruker)

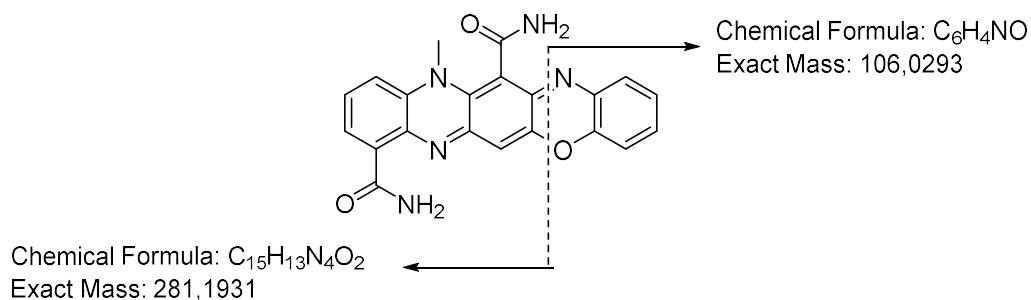
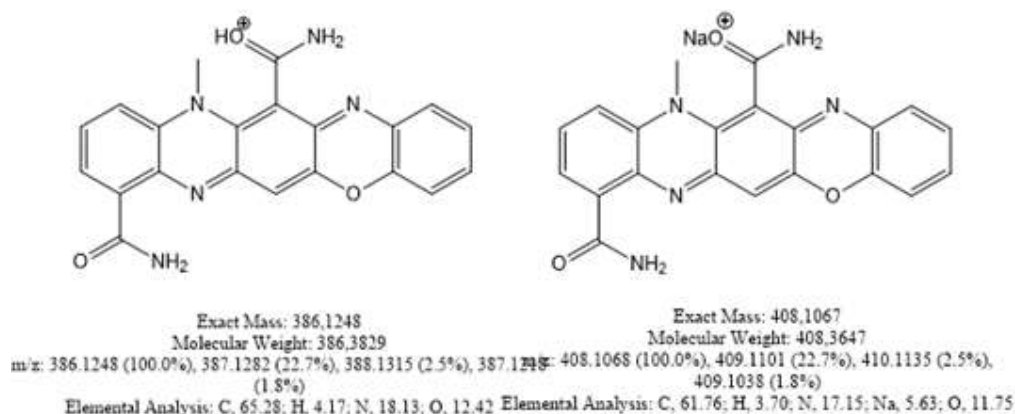
Bertalan Juhasz et al.


Figure S3A. Proposed MS fragmentation pathway of dermacozine N (**1**) showing loss of a (-ON(C₆H₄)-) fragment.



$$\text{ME C21H16N5O3} = ([\text{M}+\text{H}]^+_{\text{QTOF}} - [\text{M}+\text{H}]^+_{\text{Calculated}})/[\text{M}+\text{H}]^+_{\text{QTOF}} = -0.259 \text{ ppm}$$

$$\text{ME C21H15N5O3Na} = ([\text{M}+\text{Na}]^+_{\text{QTOF}} - [\text{M}+\text{Na}]^+_{\text{Calculated}})/[\text{M}+\text{Na}]^+_{\text{QTOF}} = 0 \text{ ppm}$$

$$m/z^+ [\text{M}+\text{H}]^+_{\text{QTOF}} = 386.1247$$

$$m/z^+ [\text{M}+\text{Na}]^+_{\text{QTOF}} = 408.1068$$

Figure S3B. Mass Error between the calculated (Chemdraw modelled) and experimental (qTOF) *m/z* ratio of dermacozine N (**1**)

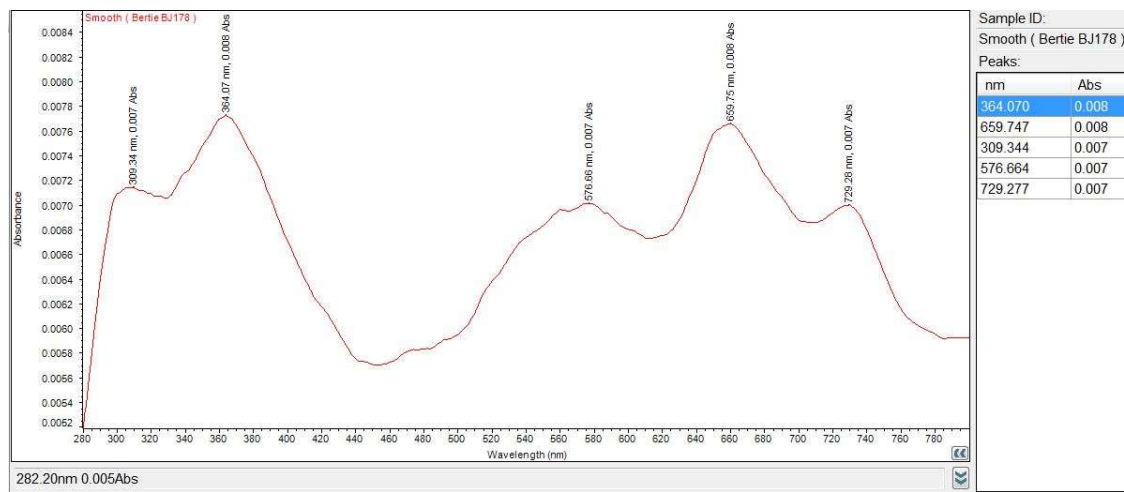
Bertalan Juhasz et al.


Figure S4. UV-Vis spectrum of dermacozine N (1) in EtOH

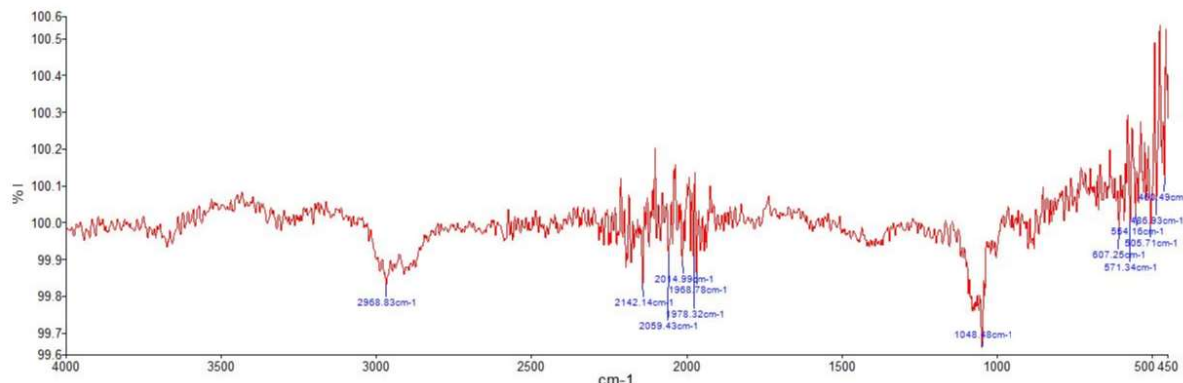
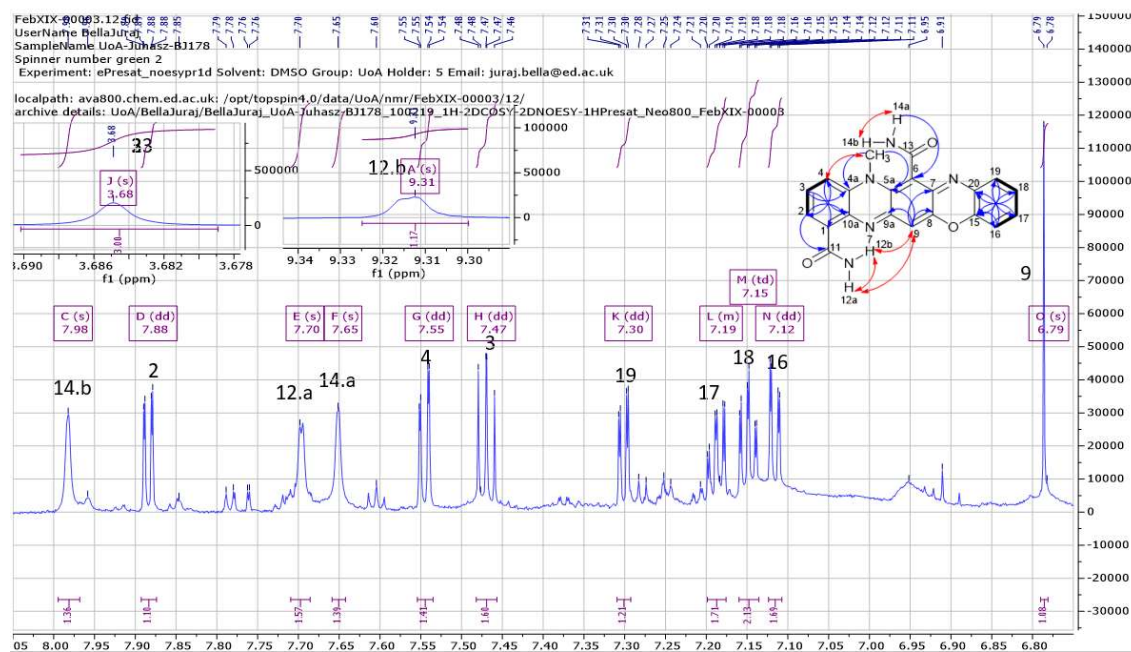
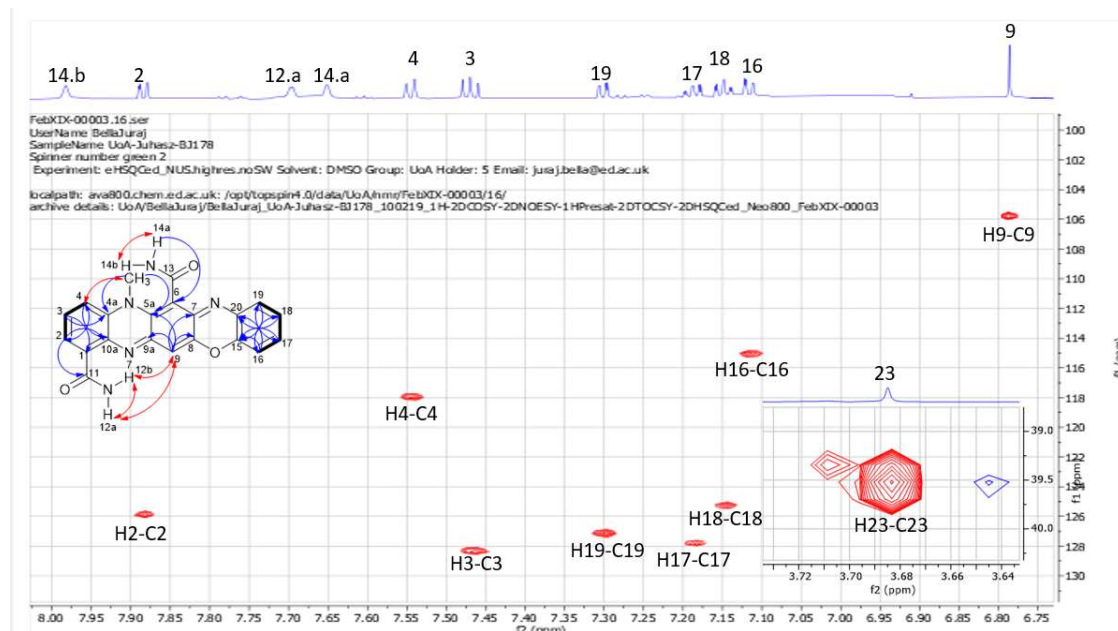


Figure S5. IR spectrum of dermacozine N (1) in EtOH



Bertalan Juhasz et al.

Figure S6. Dermacozine N (1) ^1H -NMR spectrum (800 MHz, $\text{DMSO}-d_6$)Figure S7. ^1H - ^{13}C HSQC spectrum of dermacozine N (1) (800 MHz, $\text{DMSO}-d_6$)
(Inset shows the N-methyl group)



Bertalan Juhasz et al.

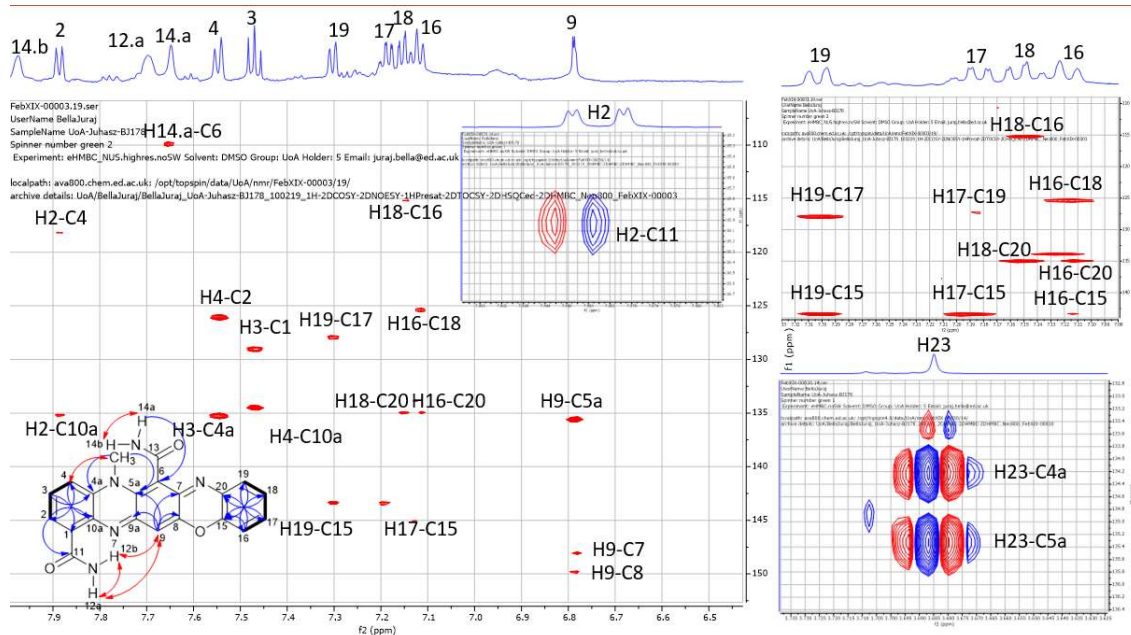


Figure S8. ^1H - ^{13}C HMBC (magnitude mode) spectrum of dermacozine N (1) (800 MHz, $\text{DMSO}-d_6$) Insets show the H-2 to C-11 carbonyl correlation (top left, phase sensitive mode), the *ortho*-substituted D-ring (top right, magnitude mode) and N-methyl C4a, C5a correlation (bottom right, phase sensitive mode)

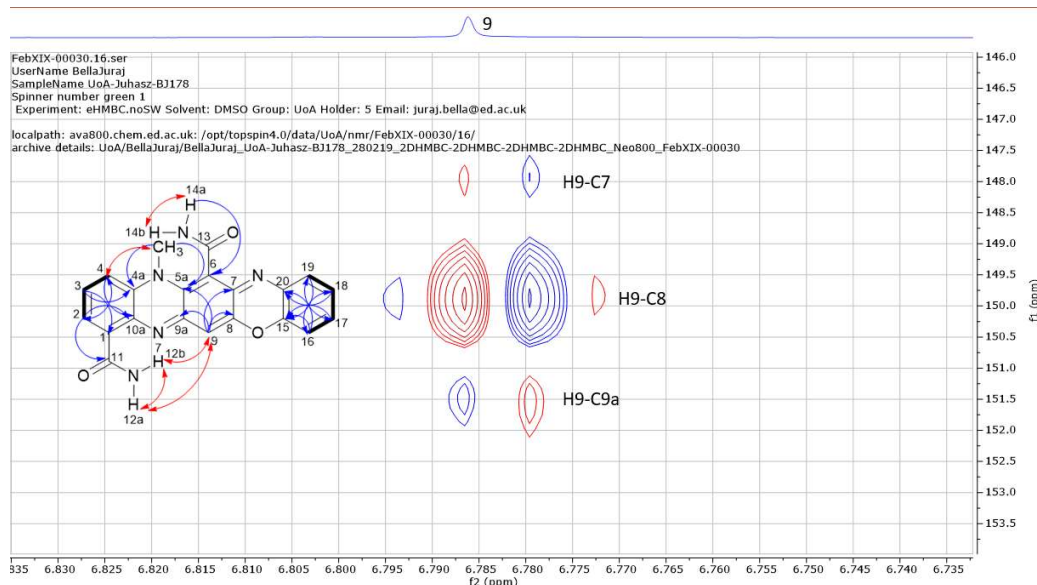


Figure S9. ^1H - ^{13}C HMBC spectrum of dermacozine N (1) with 2 Hz Coupling (800 MHz, $\text{DMSO}-d_6$)

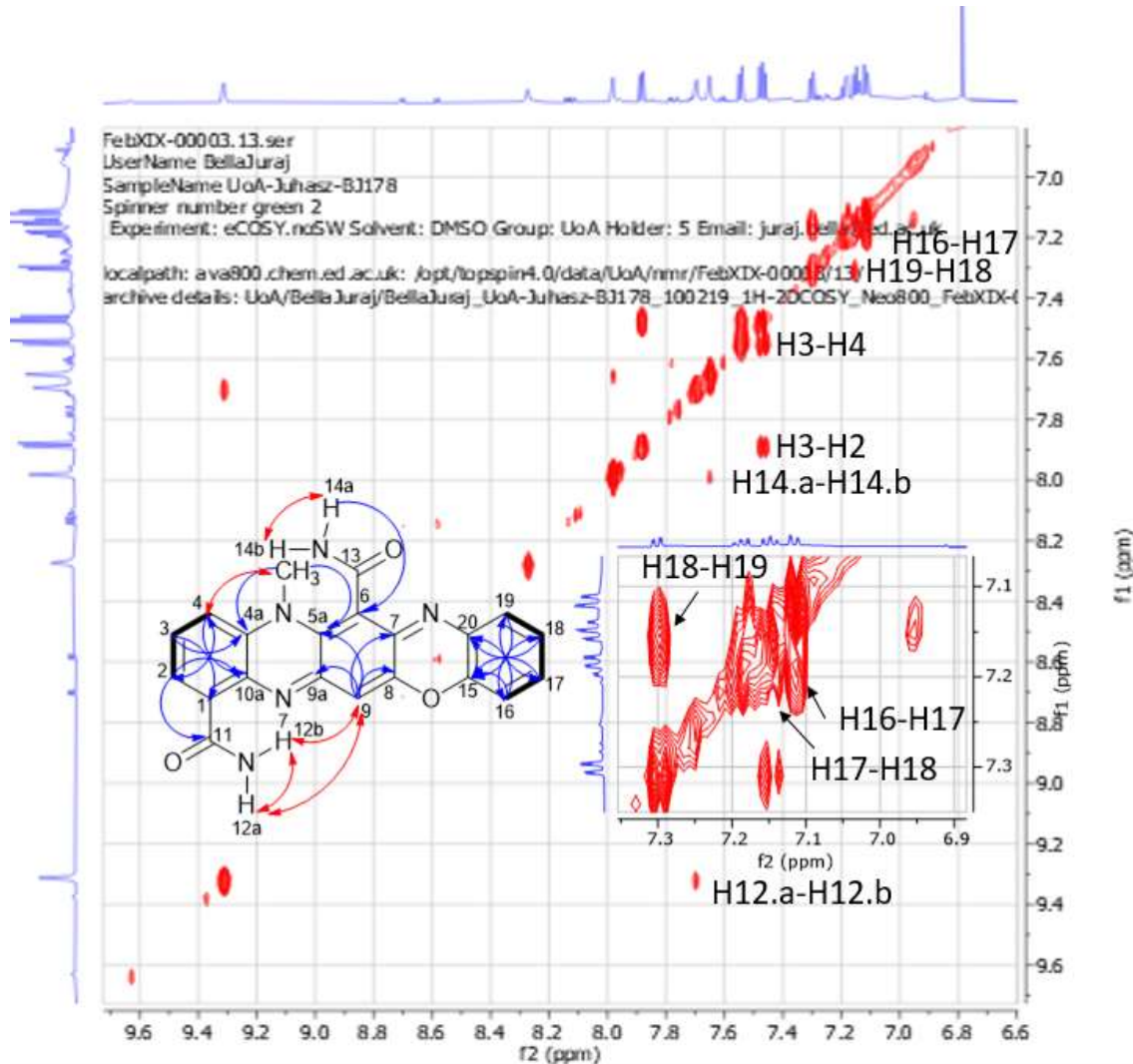
Bertalan Juhasz et al.


Figure S10. ^1H - ^1H COSY spectrum of dermacozine N (**1**) (800 MHz, $\text{DMSO}-d_6$)

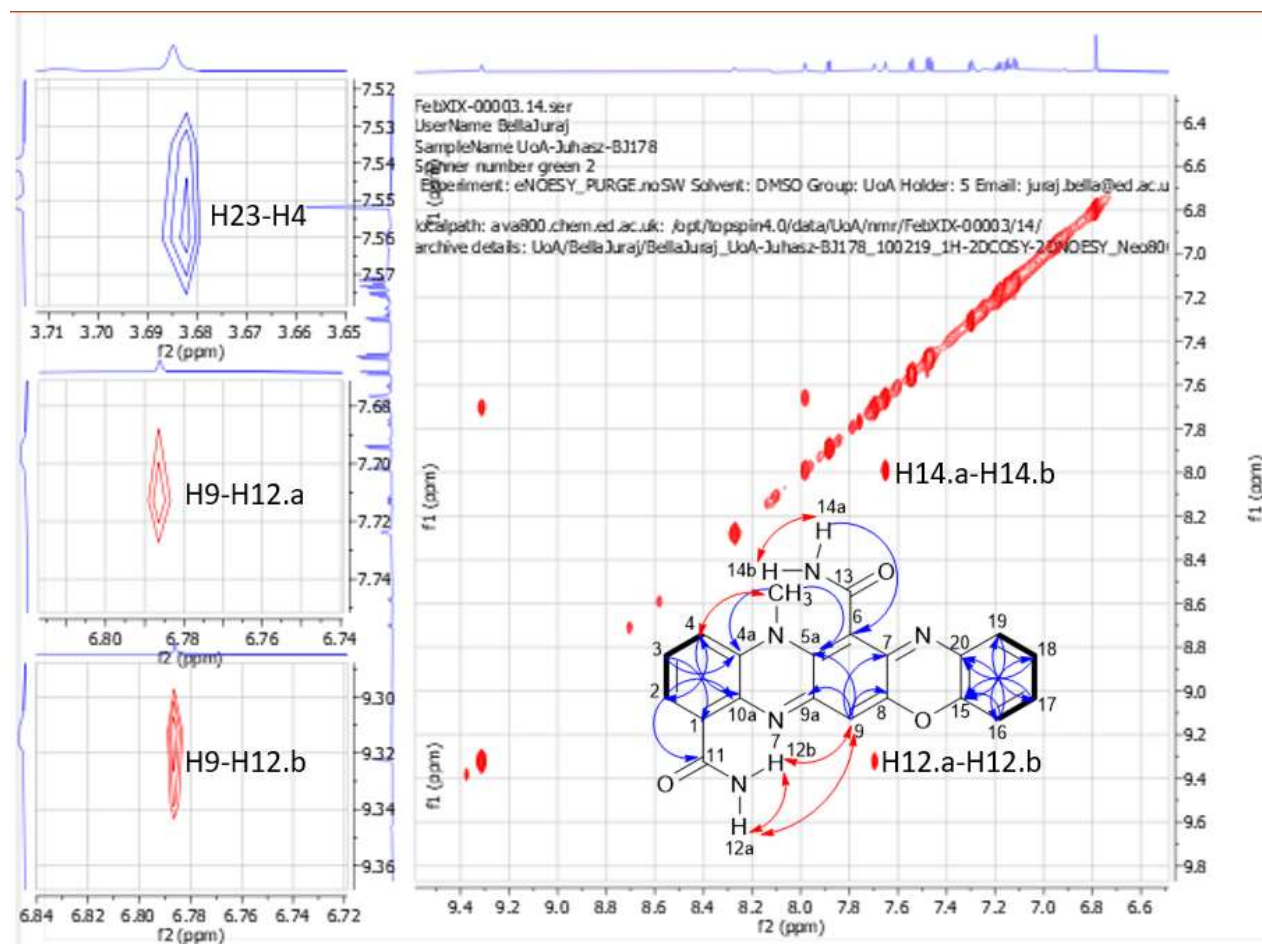
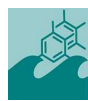
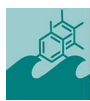


Figure S11. ¹H-¹H NOESY spectrum of dermacozine N (1) (800 MHz, DMSO-*d*₆)
(Inlets show the N-methyl and H-4 (top), and NH₂-12 to H-9 (middle and lower) correlations)



Bertalan Juhasz et al.

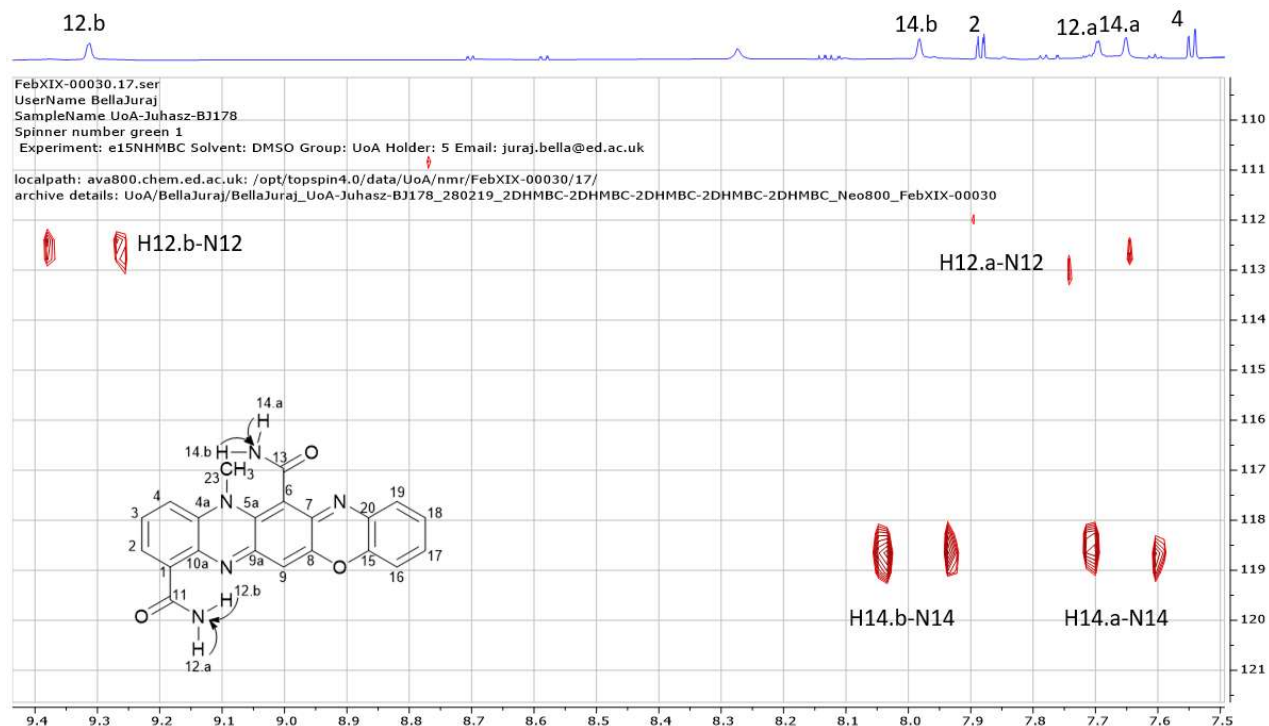
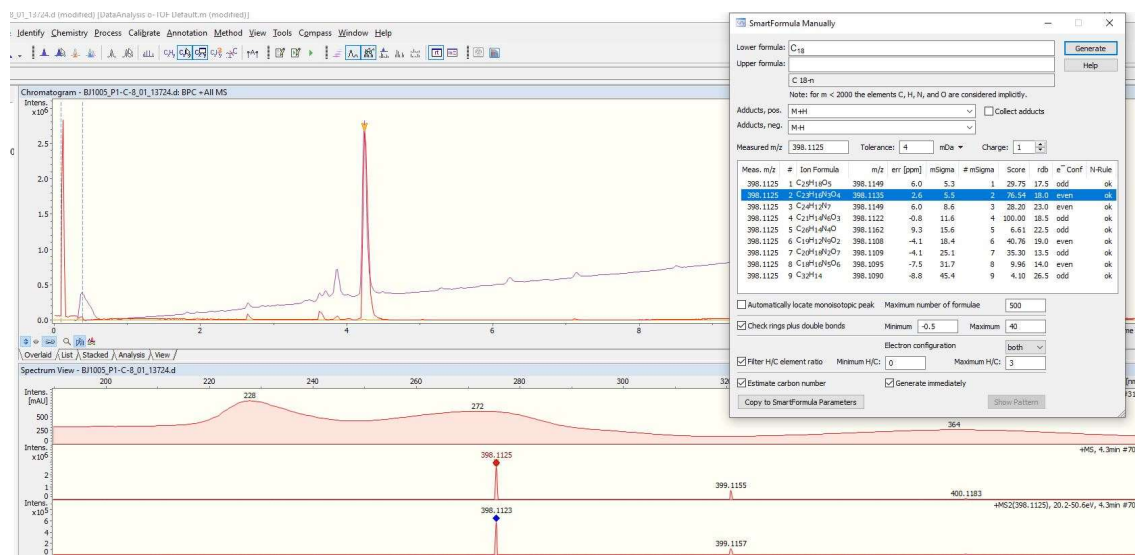
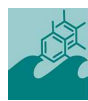
Figure S12. ¹H-¹⁵N HMBC spectrum of dermacozine N (1) (800 MHz, DMSO-*d*₆)

Figure S13. LC-MS analysis of dermacozine O (2) (qTOF, Bruker)



Bertalan Juhasz et al.

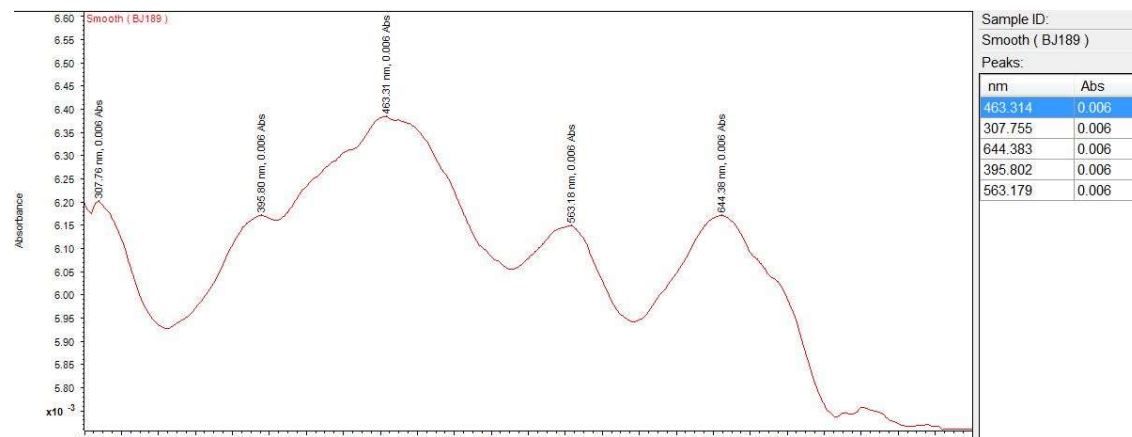


Figure S14. UV-Vis spectrum of dermacozine O (2) in EtOH

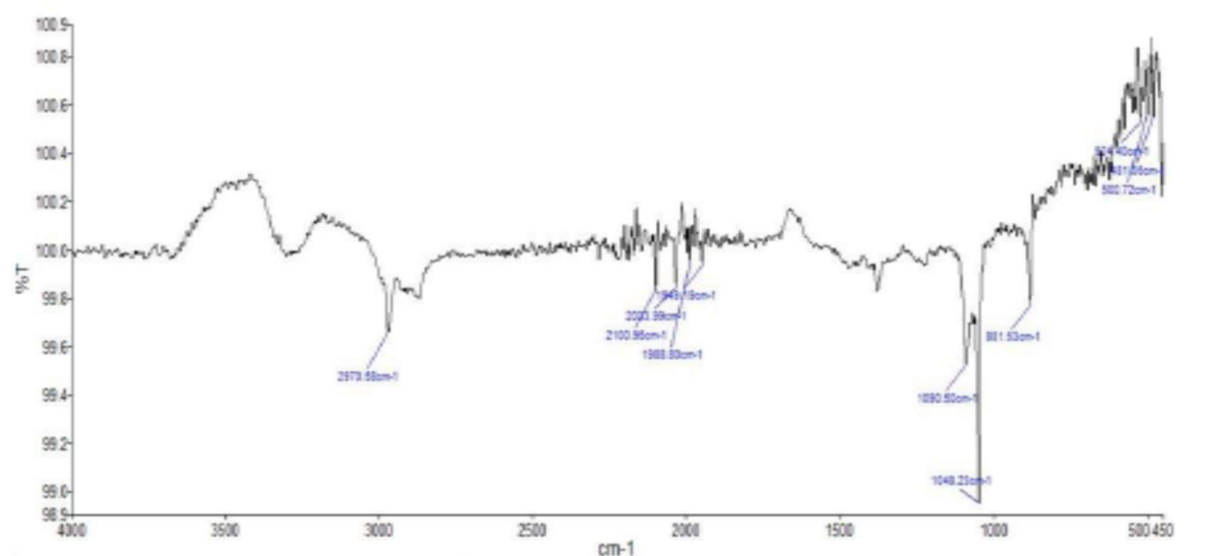


Figure S15. IR spectrum of dermacozine O (2) in EtOH

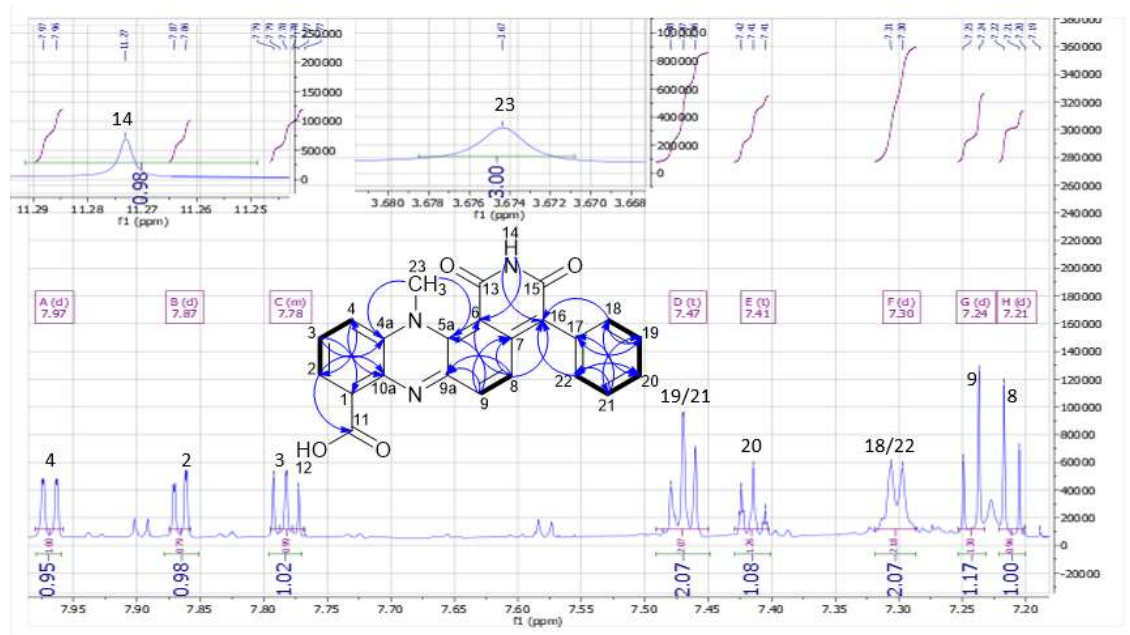


Figure S16. ^1H -NMR spectrum of dermacozine O (**2**) (800 MHz, $\text{DMSO}-d_6$)

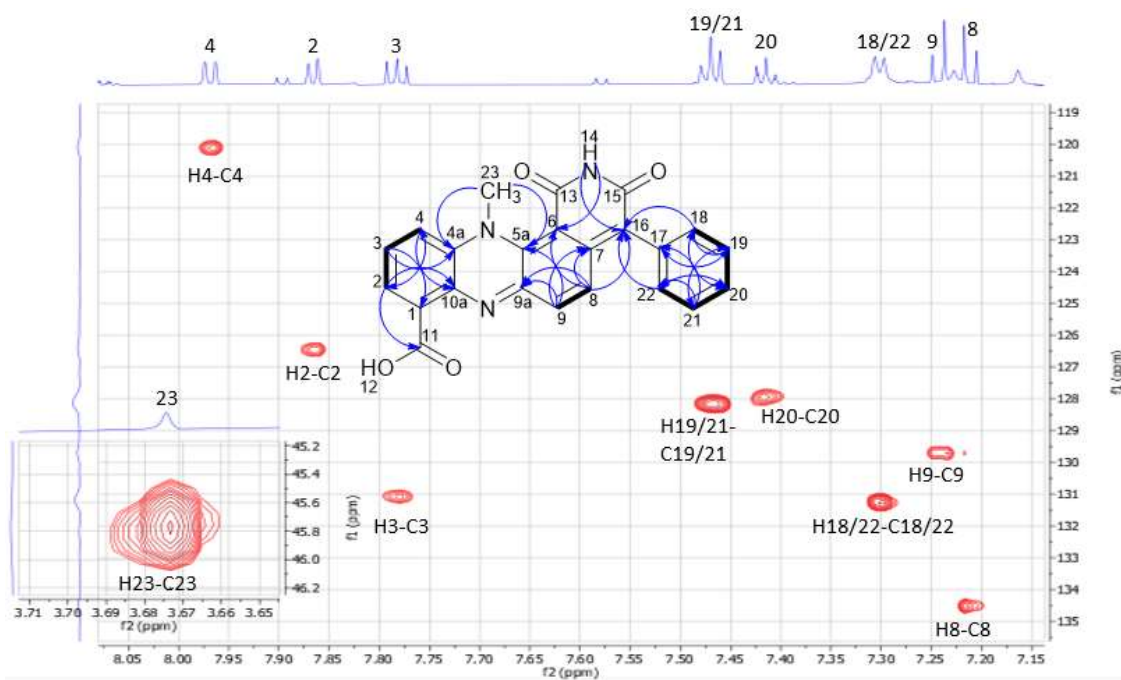
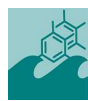


Figure S17. ^1H - ^{13}C HSQC spectrum of dermacozine O (**2**) (800 MHz, $\text{DMSO}-d_6$)



Bertalan Juhasz et al.

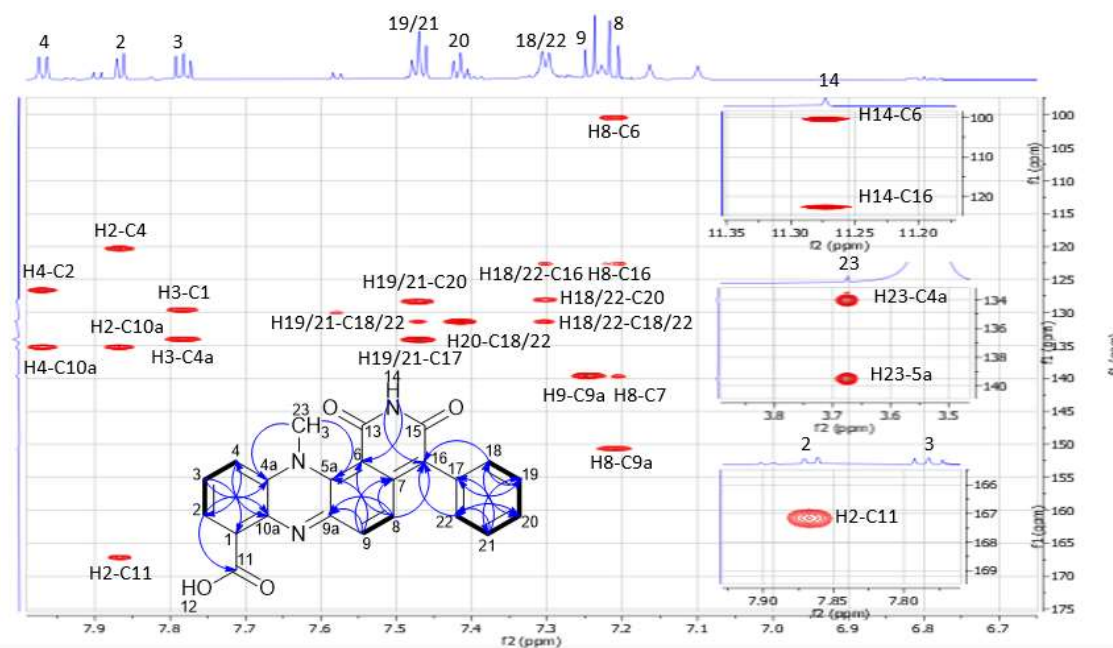


Figure S18. ^1H - ^{13}C HMBC spectrum of dermacozine O (2) (800 MHz, $\text{DMSO}-d_6$)
(Inlets show NH-14 and C-6, C-16 correlations (top), N-methyl hydrogen atom to C4a and C5a correlations (middle), H2 to C-11 carbonyl correlation (bottom))

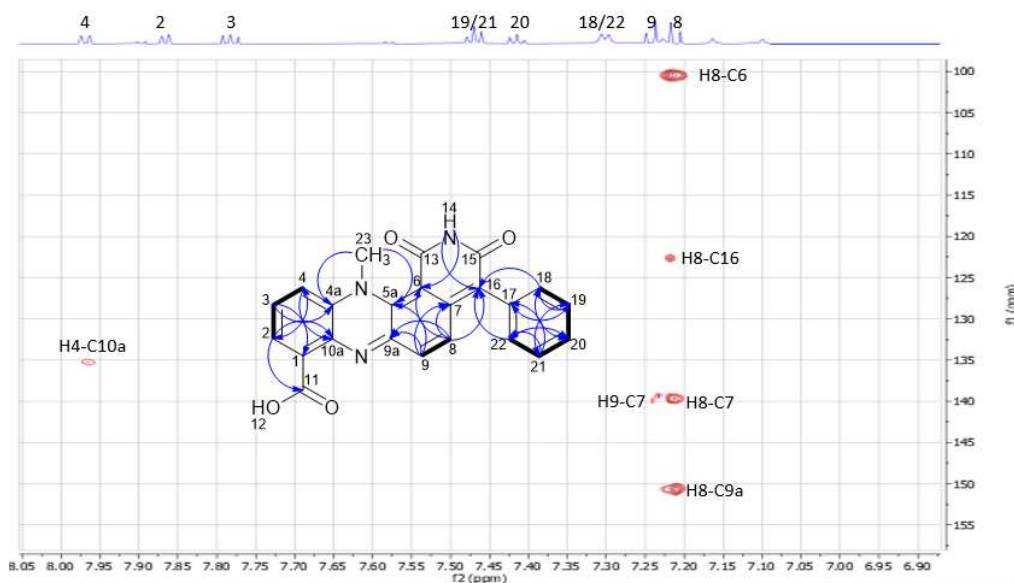
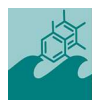


Figure S19. Long Range ^1H - ^{13}C HMBC correlations of Dermacozine O (2) with $J = 2\text{ Hz}$ (800 MHz, $\text{DMSO}-d_6$)



Bertalan Juhasz et al.

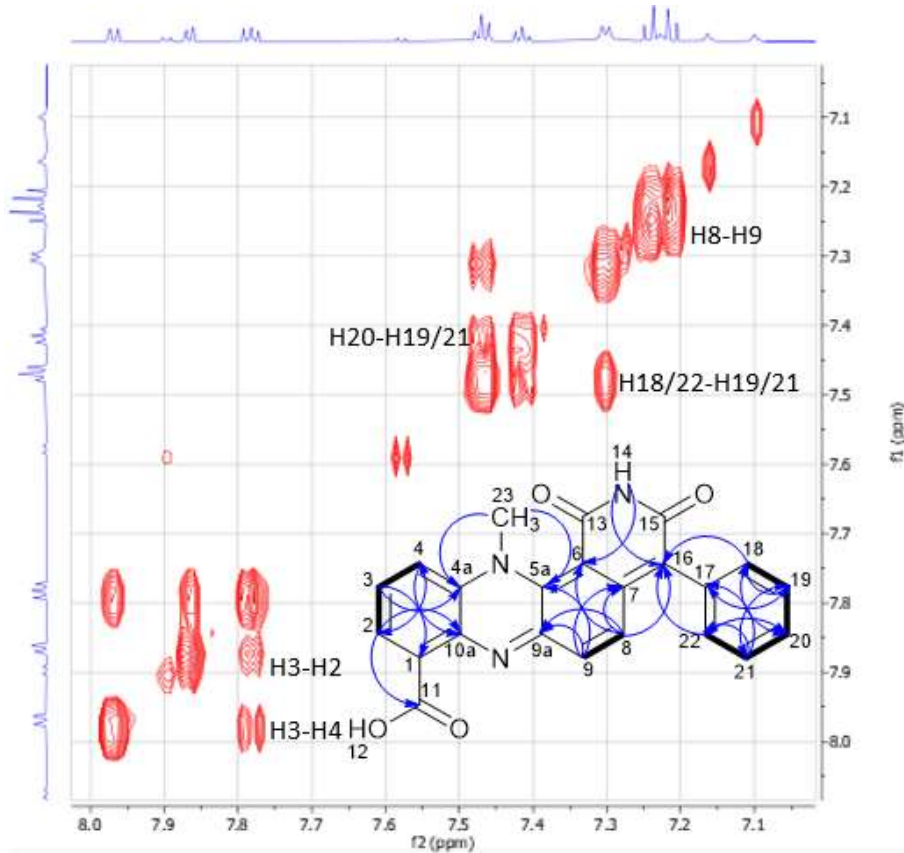


Figure S20. ^1H - ^1H COSY spectrum of dermacozine O (2) (800 MHz, $\text{DMSO}-d_6$)

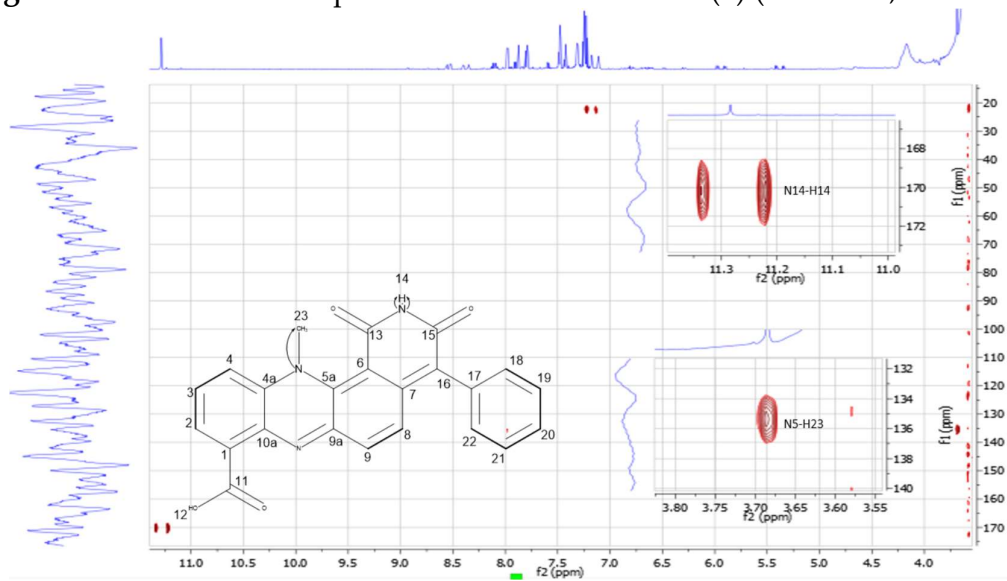


Figure S21. ^1H - ^{15}N HMBC spectrum of dermacozine O (2) (800 MHz, $\text{DMSO}-d_6$)
Inlets show the N-methyl nitrogen (top) and the cyclic carboximide nitrogen (bottom)

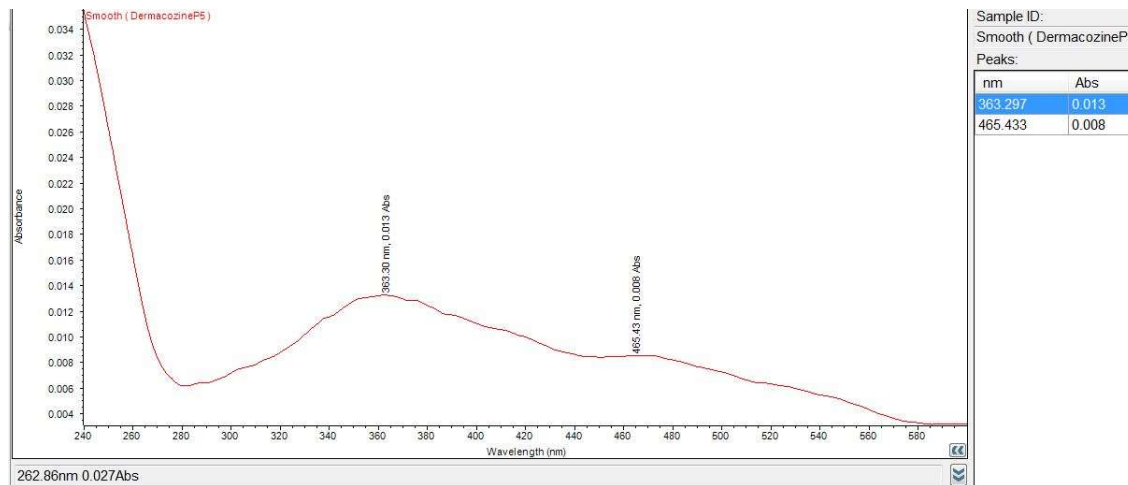
Bertalan Juhasz et al.


Figure S22. UV-Vis spectrum of dermacozine P (3) in EtOH

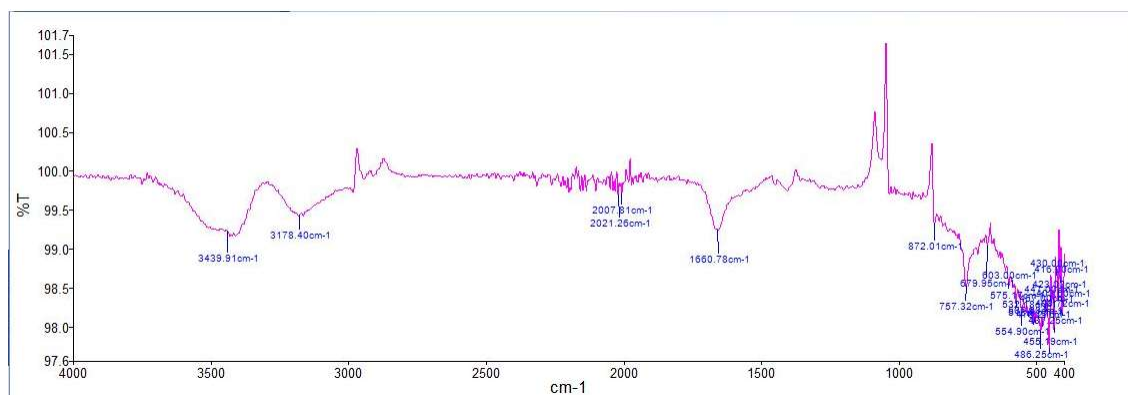
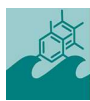


Figure S23. IR spectrum of dermacozine P (3) in EtOH



Bertalan Juhasz et al.

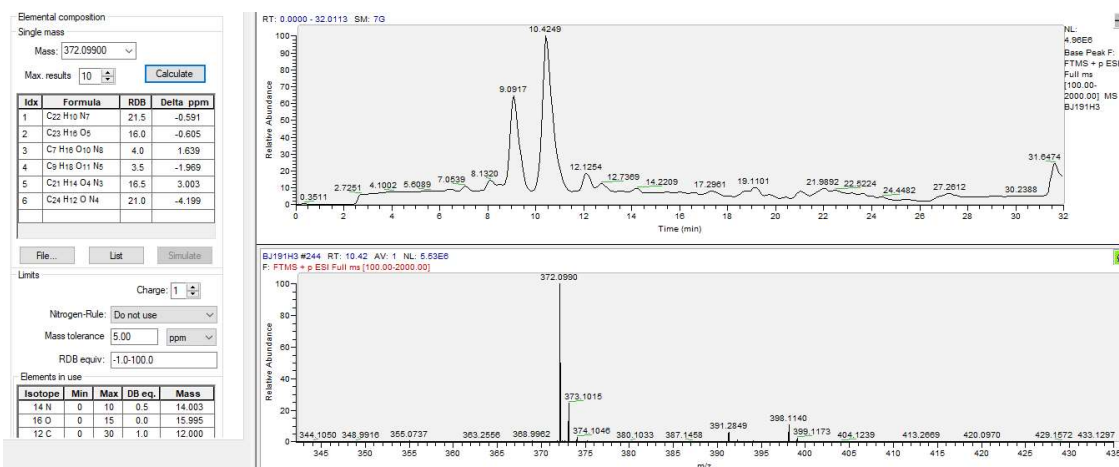


Figure S24. LC-MS analysis of dermacozine P (3) (Orbitrap, Xcalibur)

BJ191H3 #239-426 RT: 10.29-17.50 AV: 3 NL: 1.53E5
T: Average spectrum MS2 372.10 (239-426)

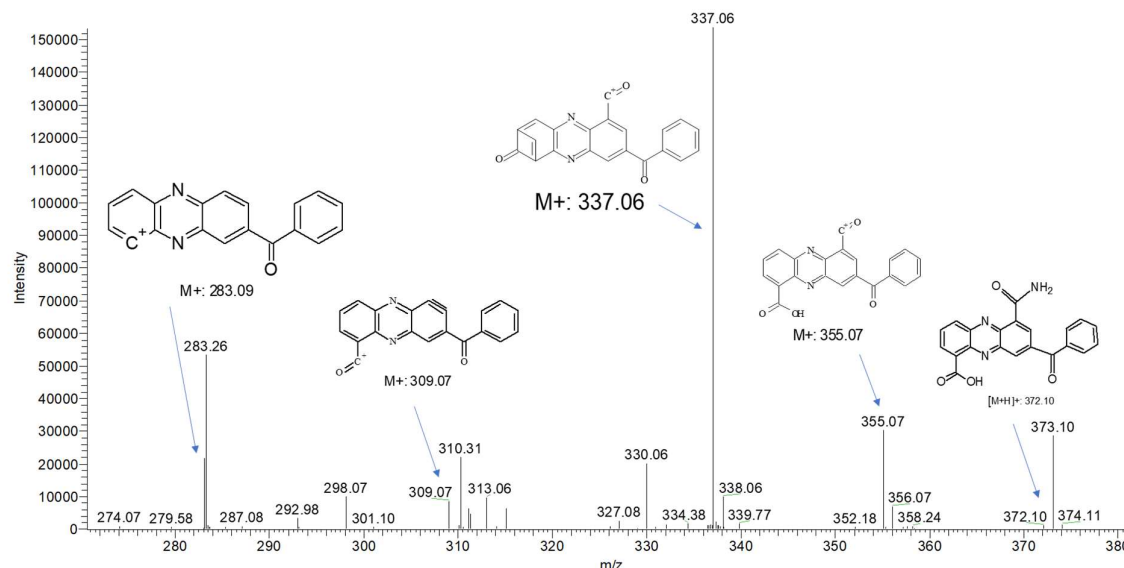


Figure S25. MS/MS analysis of dermacozine P (3) (Orbitrap, Xcalibur)

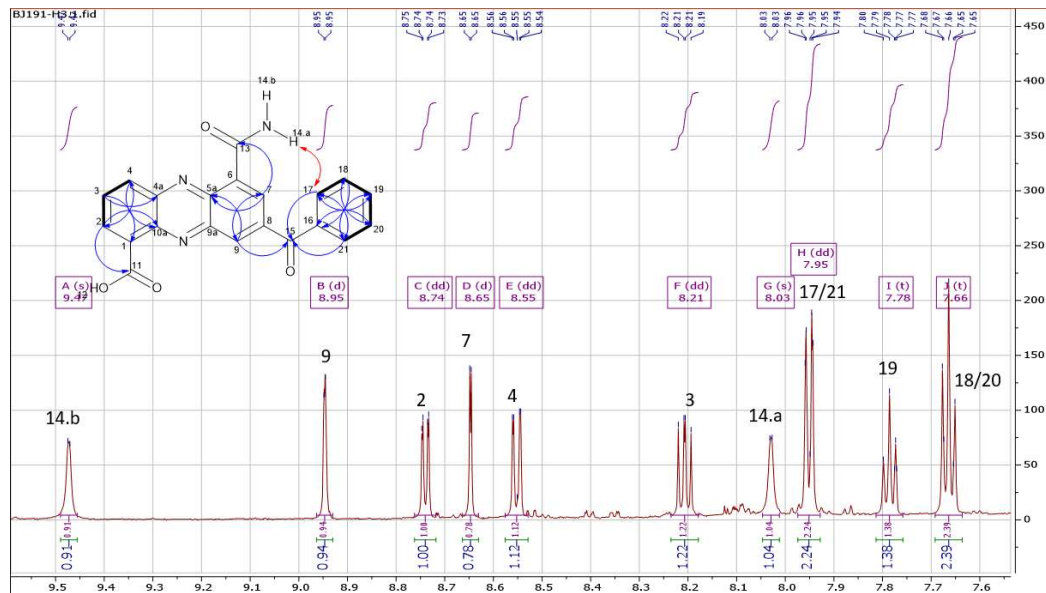
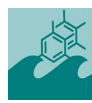


Figure S26. ^1H -NMR spectrum of dermacozine P (3) (600 MHz, $\text{DMSO}-d_6$)

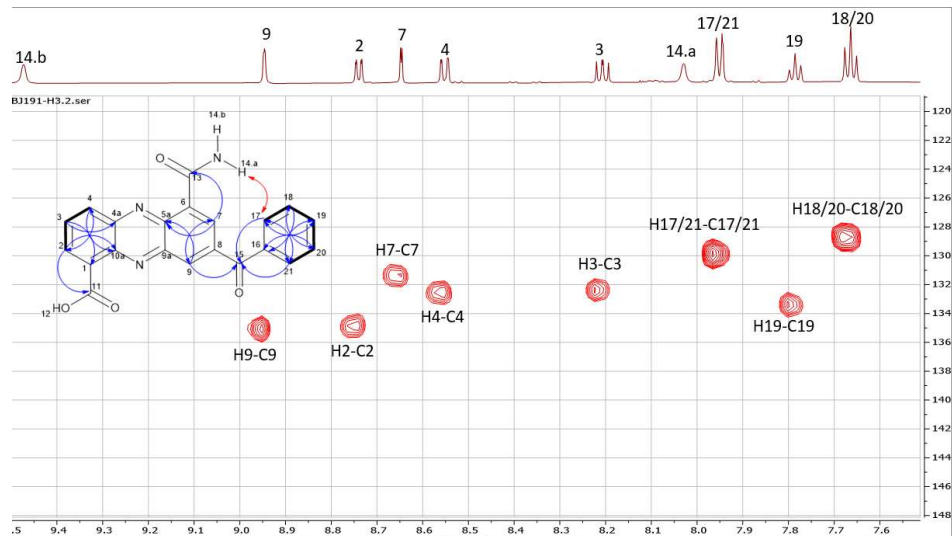
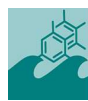


Figure S27. ^1H - ^{13}C HSQC spectrum of dermacozine P (3) (600 MHz, $\text{DMSO}-d_6$)



Bertalan Juhasz et al.

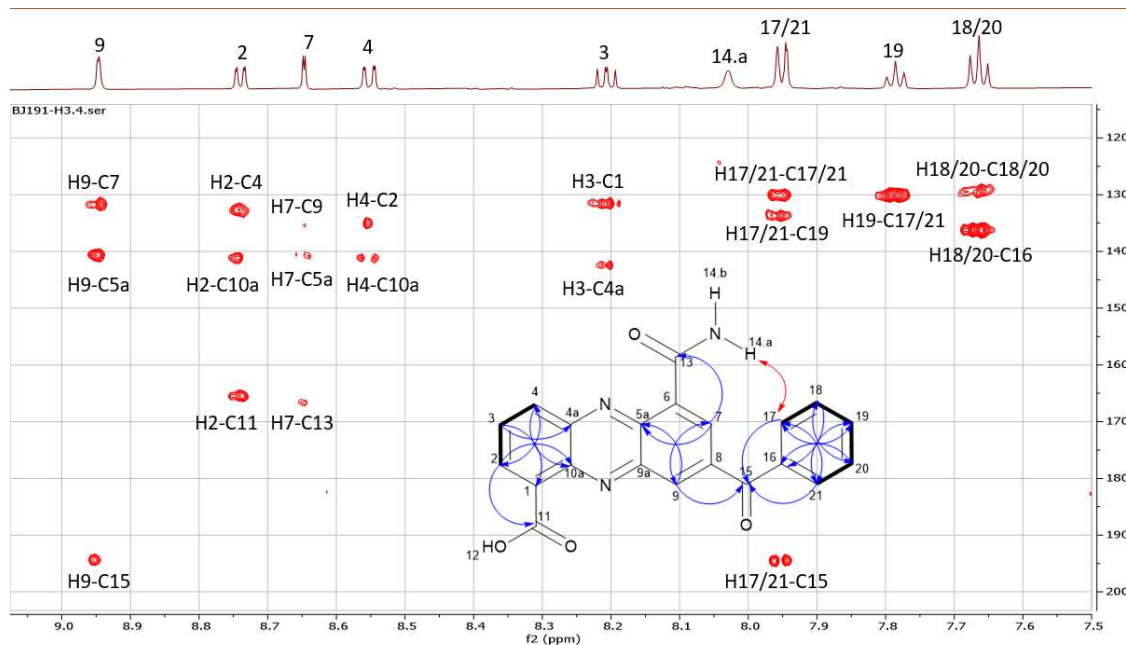


Figure S28. ^1H - ^{13}C HMBC spectrum of dermacozine P (3) (600 MHz, DMSO- d_6)

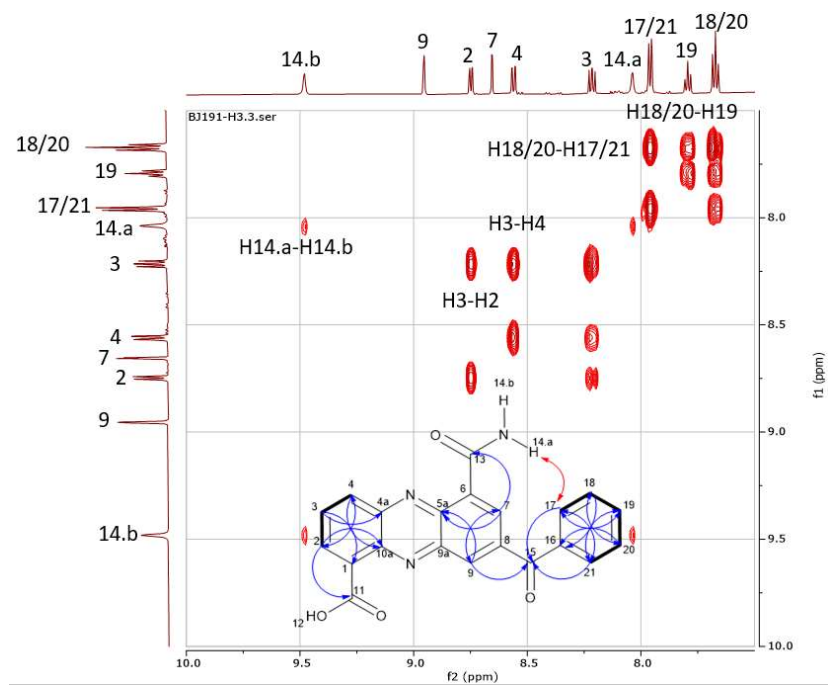


Figure S29. ^1H - ^1H COSY spectrum of dermacozine P (3) (600 MHz, DMSO- d_6)

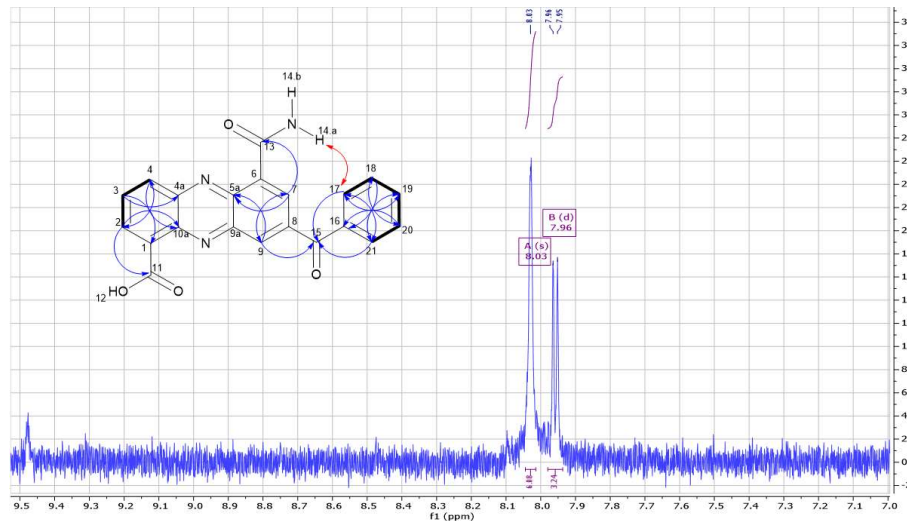
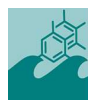


Figure S30. 1D-NOESY spectrum of dermacozine P (**3**) (600 MHz, $\text{DMSO}-d_6$) from irradiation of the signal at 8.03 ppm.

Dermacozine A-D δ_{C} shifts modelled with ACD Labs Neural Network Algorithm

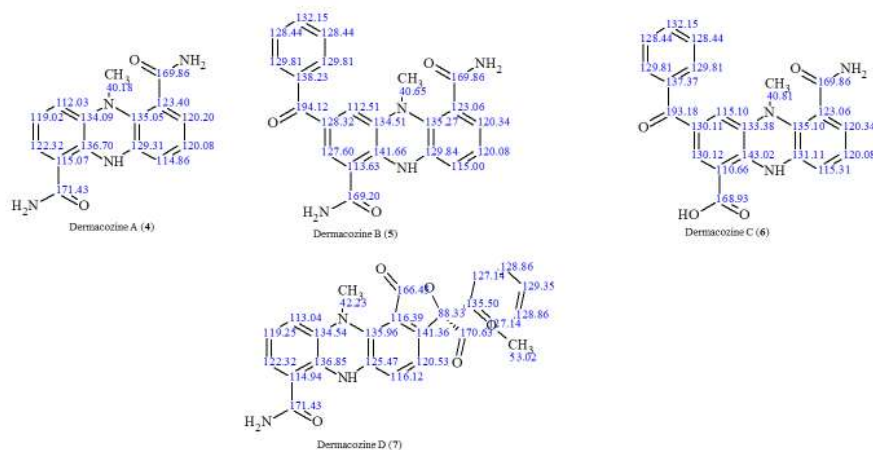
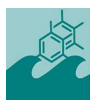


Figure S31. ^{13}C -NMR δ calculated values of dermacozine A-D (**4-7**) using the ACD Labs software with Neural Network Algorhitm Algorithm, solvent $\text{DMSO}-d_6$



Bertalan Juhasz et al.

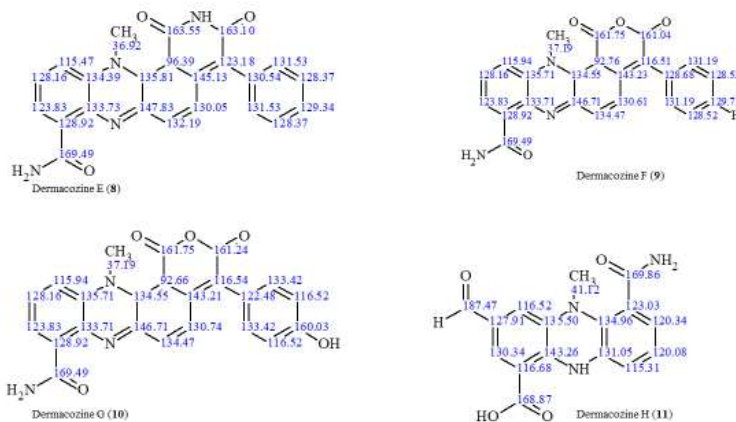
Demarcozine E-H δ_{C} shifts modelled with ACD Labs Neural Network Algorithm

Figure S32. ^{13}C -NMR δ calculated values of dermacozine E-H (**8-11**) using the ACD Labs Software with Neural Network Algorhitm Algorithm, solvent DMSO- d_6

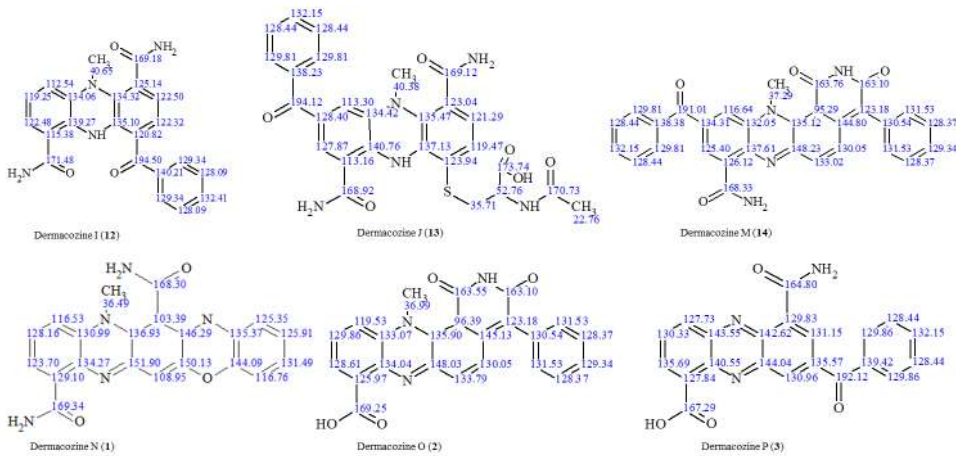
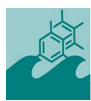
Demarcozine I-J and dermacozine M-P δ_{C} shifts modelled with ACD Labs Neural Network Algorithm

Figure S33. ^{13}C -NMR δ calculated values of dermacozine I-J (**12-13**) and dermacozine M-P (**14, 1-3**) using the ACD Labs Software with Neural Network Algorhitm Algorithm, solvent DMSO- d_6



Bertalan Juhasz et al.

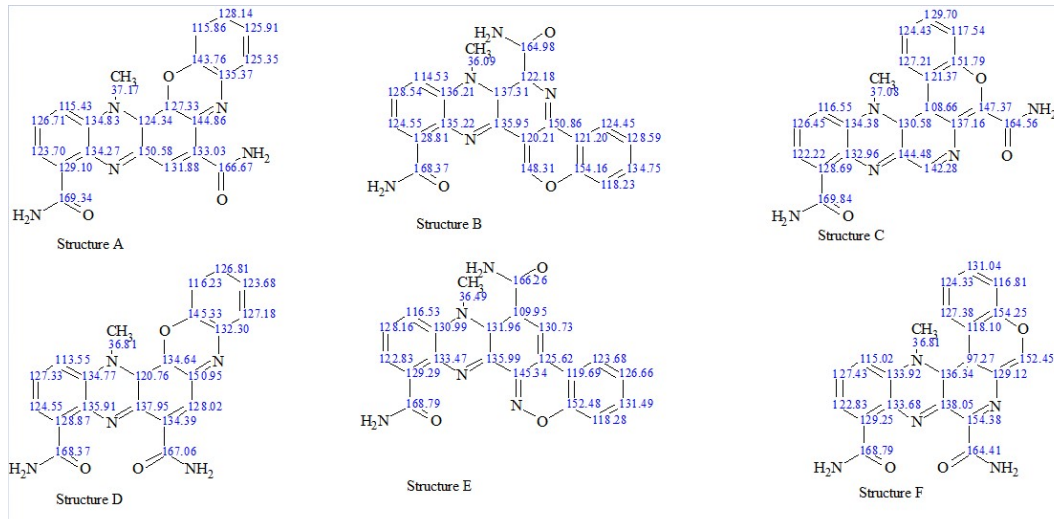


Figure S34. ^{13}C -NMR δ calculated values of possible structures (A-F) of dermacozine N (1), using the ACD Labs Software with Neural Network Algorhitm Algorithm, solvent DMSO- d_6

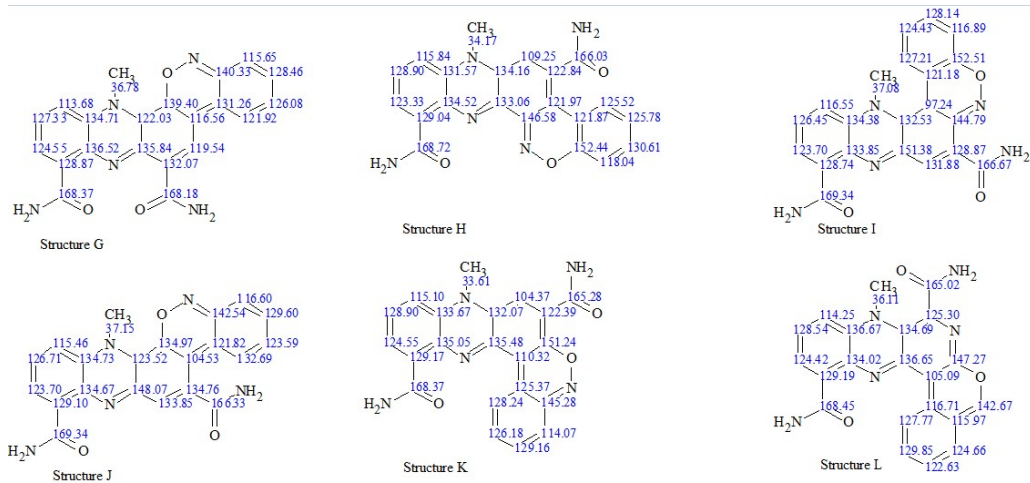


Figure S35. ^{13}C -NMR δ calculated values of possible structures (G-L) of dermacozine N (1), using the ACD Labs Software with Neural Network Algorhitm Algorithm, solvent DMSO- d_6



Bertalan Juhasz et al.

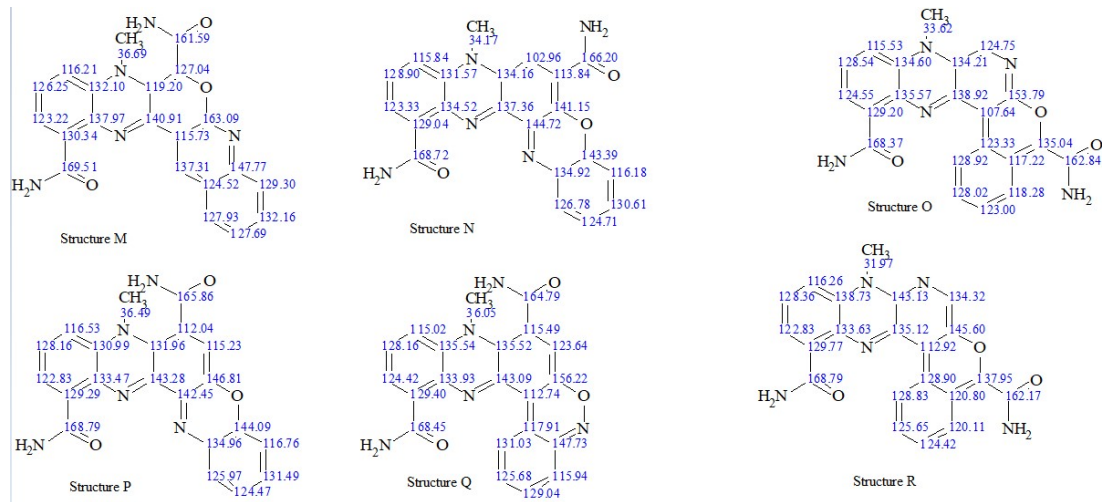


Figure S36. ^{13}C -NMR δ calculated values of possible structures (M-R) of dermacozine N (1), using the ACD Labs Software with Neural Network Algorithm, solvent DMSO-*d*

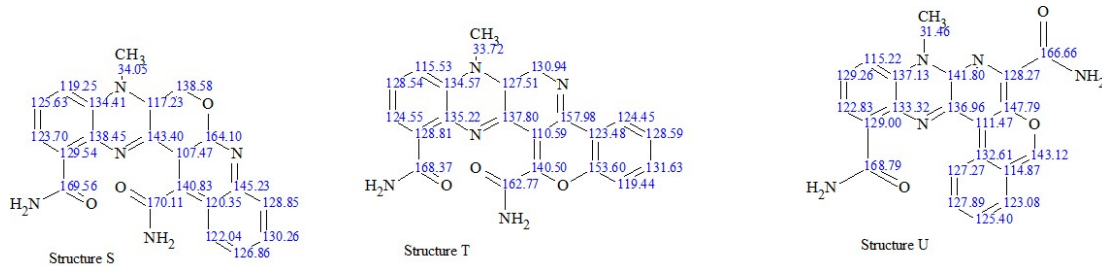
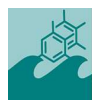


Figure S37. ^{13}C -NMR δ calculated values of possible structures (S-U) of dermacozine N (1), using the ACD Labs Software with Neural Network Algorithm, solvent DMSO-*d*



Bertalan Juhasz et al.

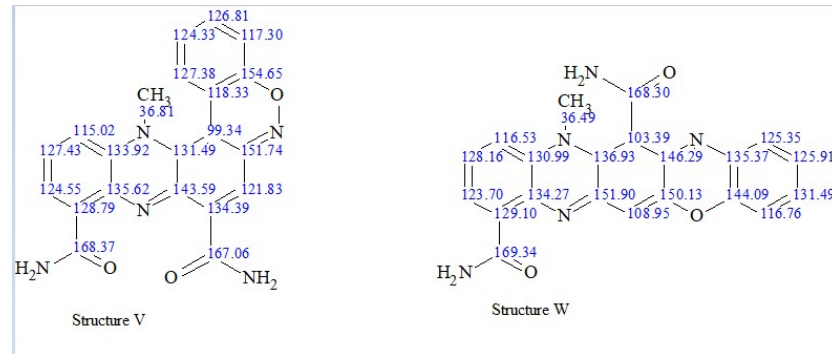


Figure S38. ^{13}C -NMR δ calculated values of possible structures (**V** and **W**) of dermacozine N (**1**), using the ACD Labs Software with Neural Network Algorithm, solvent DMSO-*d*₆



Dermazine Atom Number	Dermazine A	Experimental $\delta^{13}\text{C}$	Calculated $\delta^{13}\text{C}$	Dermazine B	Experimental $\delta^{13}\text{C}$	Calculated $\delta^{13}\text{C}$	Dermazine C	Experimental $\delta^{13}\text{C}$	Calculated $\delta^{13}\text{C}$	Dermazine D	Experimental $\delta^{13}\text{C}$	Calculated $\delta^{13}\text{C}$	Dermazine E	Experimental $\delta^{13}\text{C}$	Calculated $\delta^{13}\text{C}$	Dermazine F	Experimental $\delta^{13}\text{C}$	Calculated $\delta^{13}\text{C}$	Dermazine G	Experimental $\delta^{13}\text{C}$	Calculated $\delta^{13}\text{C}$	Dermazine H	Experimental $\delta^{13}\text{C}$	Calculated $\delta^{13}\text{C}$	Dermazine I					
1	113	151	112	116	104	107	109	119	117	129	119	128	131	129	129	121	128	122	123	121	129	122	111	116	114	110	112			
2	112	123	123	126	125	129	131	123	121	123	121	128	123	123	123	121	128	123	123	123	123	123	123	125	125	123	129			
3	119	120	124	123	129	131	102	113	137	122	129	122	129	122	129	122	122	129	122	122	129	122	122	122	122	122	124			
4	150	120	147	115	143	151	114	130	136	155	195	159	197	159	195	159	195	159	195	159	195	159	195	159	195	159	193			
4	138	141	139	135	138	134	137	145	137	134	138	138	137	134	138	137	136	137	136	137	136	135	135	135	134	134	134			
5	133	151	135	133	133	151	134	130	138	149	146	147	146	130	130	130	130	130	130	130	130	130	130	130	133	134	135			
6	125	124	127	121	126	121	109	114	93	94	92	93	94	92	92	92	92	93	92	92	92	92	92	92	92	92	92	92		
7	125	122	129	103	123	103	143	144	136	151	147	142	145	142	142	142	142	142	142	142	142	142	142	142	125	125	123			
8	126	121	119	121	126	121	113	105	133	131	124	126	127	127	127	127	127	127	127	127	127	127	127	127	125	125	123			
9	137	149	148	150	153	153	112	111	122	134	145	129	145	122	122	122	122	122	122	122	122	122	122	122	122	122	122	122		
9	130	123	153	138	145	131	136	125	192	193	194	167	193	167	167	167	167	167	167	167	167	167	167	167	165	165	163	171		
10	146	137	146	147	147	140	149	139	137	134	137	134	137	137	137	137	137	137	137	137	137	137	137	137	137	137	137	137		
11	121	114	107	102	101	103	110	114	162	165	164	163	165	163	163	163	163	163	163	163	163	163	163	163	163	163	163	163		
12	41	42	40	47	40	48	45	42	49	39	40	43	40	37	43	37	37	37	37	37	37	37	37	37	37	37	37	37	37	44

Table S1. Comparison between calculated vs. experimental ^{13}C -NMR δ values of dermacozines A-J (4-13)

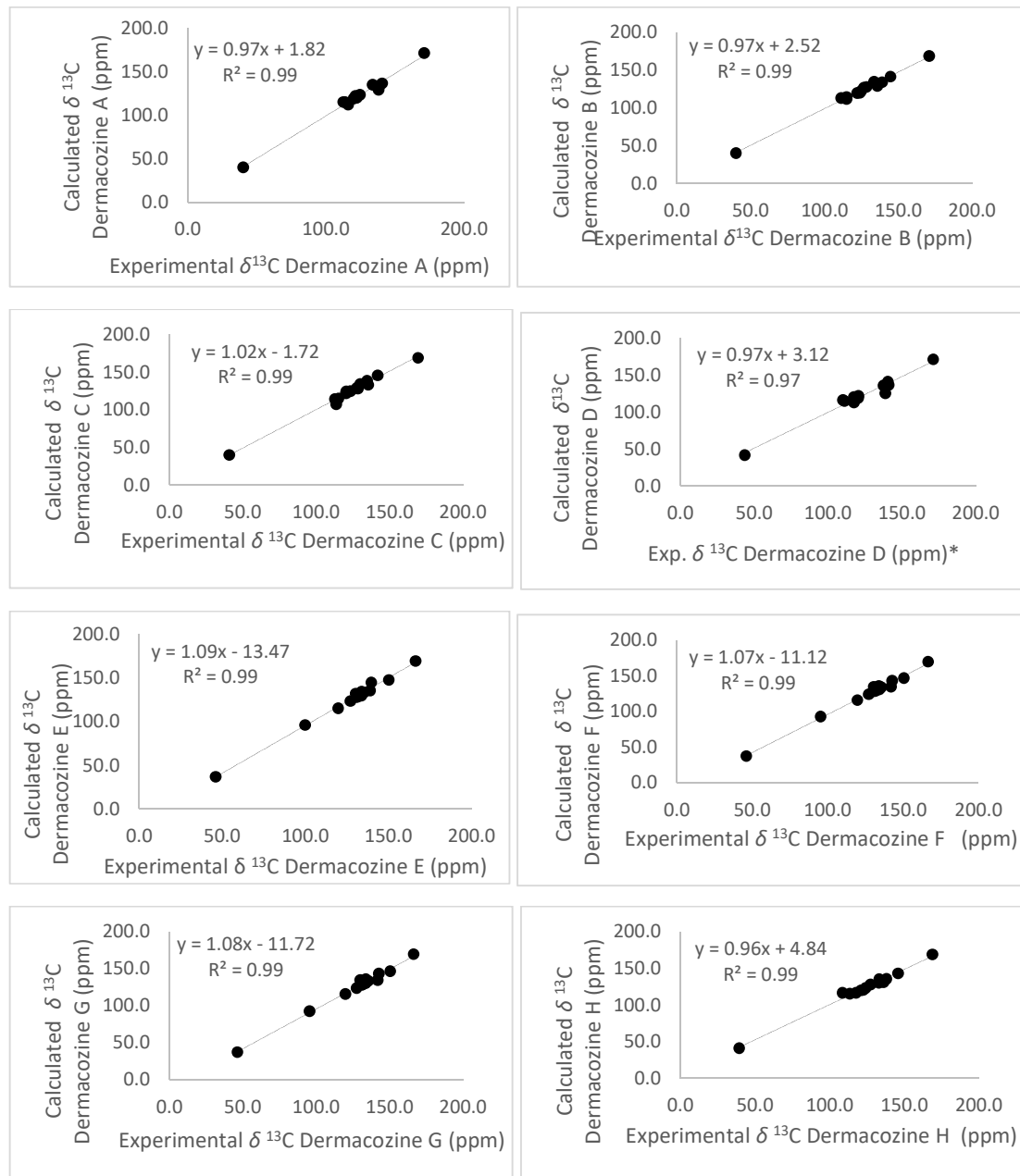
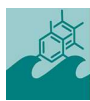


Figure 39. Linear regression graphics between ACD Labs (Neural Network Algorithm) calculated vs. experimental ^{13}C -NMR δ values of dermacozine A-H (4-11)

*Dermacozine D experimental values were recorded in Chloroform-d.

Bertalan Juhasz et al.

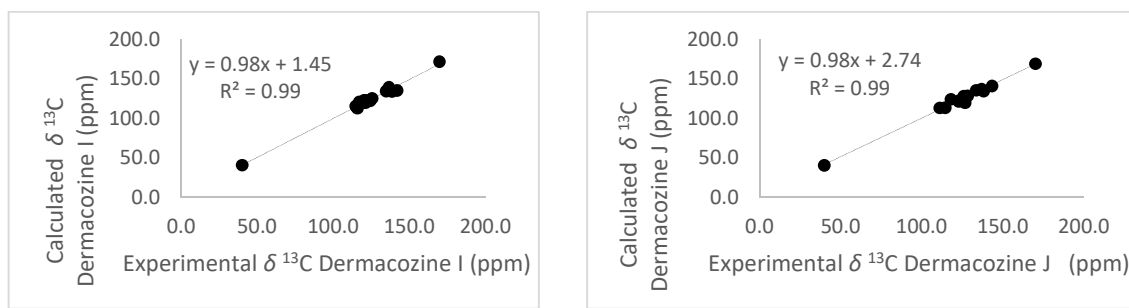
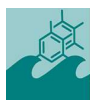


Figure 40. Linear regression graphics between ACD Labs (Neural Network Algorithm) calculated vs. experimental ^{13}C -NMR δ values of dermacozine I & J (**12-13**)



Dermacozine N Atom Numbers N	Experimental $\delta^{13}\text{C}$	Calculated $\delta^{13}\text{C}$ Structure A	Calculated $\delta^{13}\text{C}$ Structure D	Calculated $\delta^{13}\text{C}$ Structure E	Calculated $\delta^{13}\text{C}$ Structure G	Calculated $\delta^{13}\text{C}$ Structure H	Calculated $\delta^{13}\text{C}$ Structure I	Calculated $\delta^{13}\text{C}$ Structure J	Calculated $\delta^{13}\text{C}$ Structure K	Calculated $\delta^{13}\text{C}$ Structure L	Calculated $\delta^{13}\text{C}$ Structure M	Calculated $\delta^{13}\text{C}$ Structure N	Calculated $\delta^{13}\text{C}$ Structure P	Calculated $\delta^{13}\text{C}$ Structure Q	Calculated $\delta^{13}\text{C}$ Structure R	Calculated $\delta^{13}\text{C}$ Structure V	Calculated $\delta^{13}\text{C}$ Structure W	
1	128.9	129.1	128.9	129.3	128.9	129.0	128.7	129.1	128.2	129.0	129.3	129.4	128.8	128.1				
2	125.9	123.7	124.6	122.8	124.6	123.3	123.7	123.7	124.6	123.3	122.8	124.4	124.6	123.7				
3	128.4	126.7	122.3	128.2	127.3	128.9	126.5	126.7	128.9	128.9	128.2	128.2	127.4	128.2				
4	118.0	115.4	113.6	116.5	113.7	115.8	116.6	115.5	115.1	115.8	116.5	115.0	115.0	116.5				
4b	134.4	134.8	134.8	131.0	134.7	131.6	134.4	134.7	133.7	131.6	131.0	135.5	133.9	131.0				
5a	135.5	124.3	120.8	122.0	124.2	125.1	123.5	123.5	122.1	124.2	122.0	135.5	131.5	135.9				
6	109.8	127.3	134.6	110.0	139.4	108.3	97.2	97.2	135.0	108.4	108.0	120.0	115.5	99.3	108.4			
7	148.1	144.9	151.0	130.7	116.6	122.8	144.8	144.8	104.5	122.4	113.8	115.2	123.6	151.7	146.3			
8	149.8	133.0	128.0	125.6	119.5	122.0	128.9	128.9	134.8	131.2	141.2	146.8	156.2	121.8	159.1			
9	105.9	131.9	134.4	145.3	132.1	146.5	131.9	133.9	103.3	144.7	102.5	112.7	134.4	109.0				
9a	151.6	150.6	138.0	136.0	133.8	133.1	151.4	148.1	135.5	137.4	143.3	143.1	143.6	151.9				
10a	135.1	134.3	135.9	133.5	136.5	134.5	133.9	134.7	135.1	134.5	133.5	133.9	135.6	134.3				
11	165.3	169.3	168.4	168.8	166.4	168.7	169.3	169.3	168.4	168.7	168.8	168.5	168.4	169.3				
15	143.3	143.8	145.3	152.5	140.3	12.4	152.5	142.5	145.3	143.4	141.1	147.7	154.7	144.1				
16	115.0	115.9	116.2	118.3	115.7	118.0	116.9	116.6	114.1	116.2	116.8	115.9	117.3	116.8				
17	127.9	128.1	126.8	131.5	120.5	130.6	128.1	129.6	129.2	130.6	131.5	129.0	126.8	131.5				
18	125.3	125.9	123.7	126.7	126.1	125.8	124.4	123.6	126.2	124.7	124.5	125.7	125.9	125.9				
19	127.2	125.4	127.7	123.7	121.9	125.5	127.2	127.7	128.2	126.8	126.0	131.0	127.4	125.4				
20	134.8	132.3	119.7	131.3	121.9	121.2	121.8	125.4	134.9	135.0	117.9	118.3	135.4					
21	39.5	37.2	36.8	36.5	36.8	34.2	37.1	37.2	33.6	34.2	36.5	36.1	36.8	36.5				

Table S2. Comparison between the experimental ^{13}C -NMR δ values of dermacozine N (**1**) vs. the calculated ones of possible structures **A, D, E, G, H, I, J, K, N, P, Q, V, W** by ACD Labs (Neural Network Algorithm, DMSO- d_6)



Bertalan Juhasz et al.

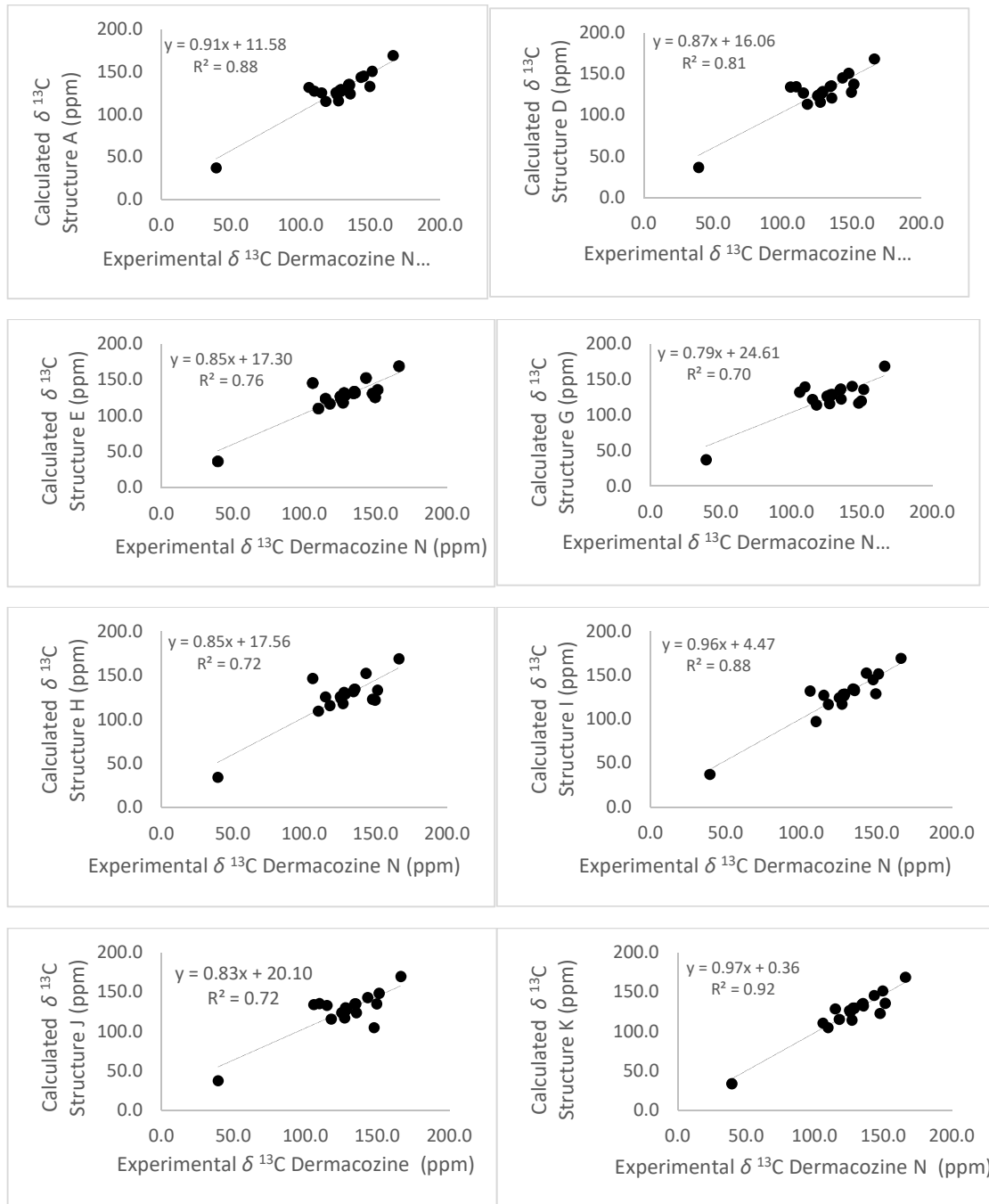


Figure S41. Linear regression graphics between ^{13}C -NMR δ experimental values of dermacozine N (1) vs. the ACD Labs calculated ones (Neural Network Algorithm, $\text{DMSO}-d_6$) (4-13)

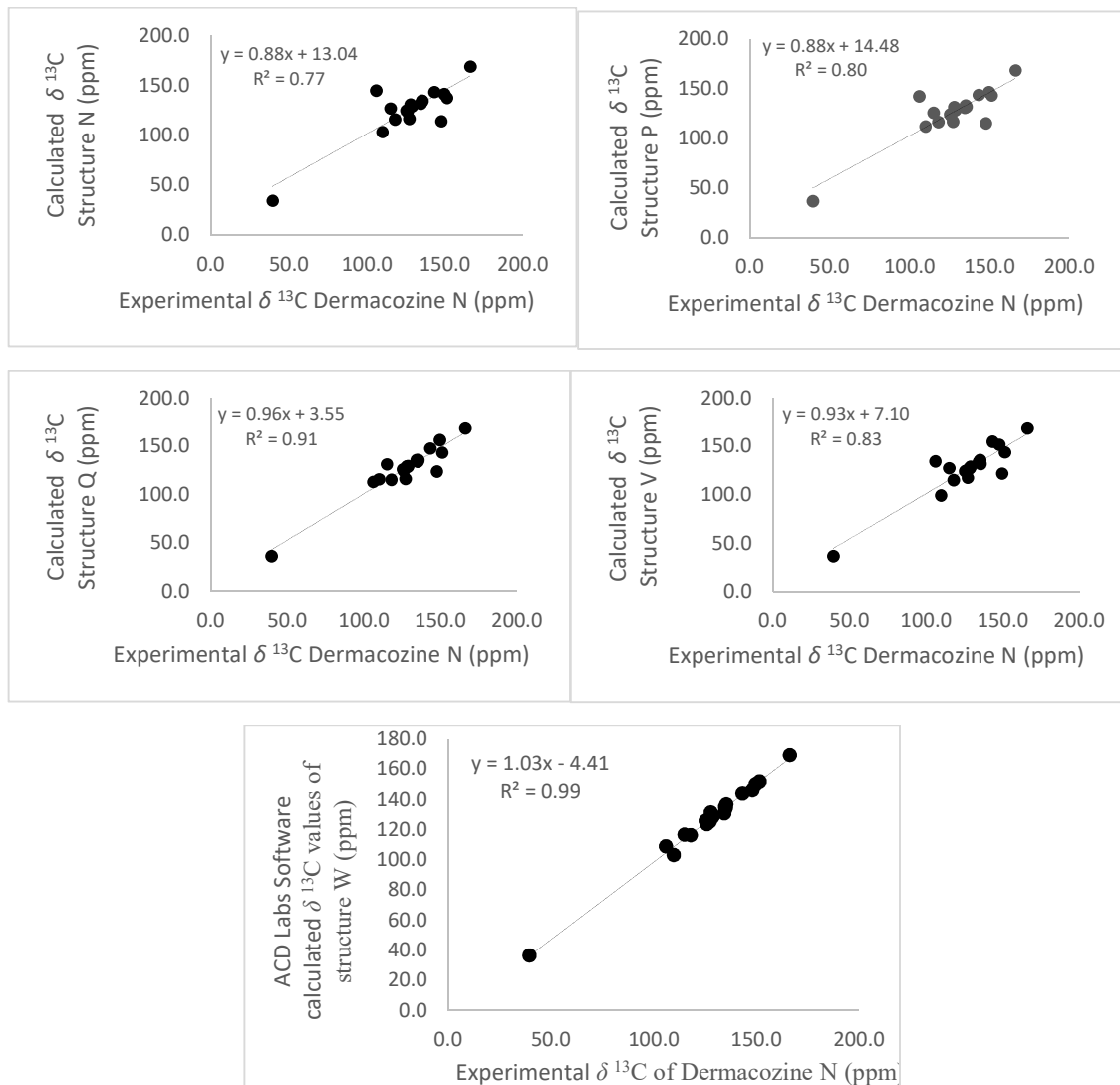
Bertalan Juhasz et al.


Figure S42. Linear regression graphics between ^{13}C -NMR δ experimental values of dermacozine N (1) vs. the ACD Labs (Neural Network Algorithm, DMSO- d_6) calculated ones for possible structures N, P, Q, V, W

Dermacozone N Atom Numbers	Experimental $\delta^{13}\text{C}$ Dermacozone N	Calculated $\delta^{13}\text{C}$ Structure W	Absolute error between the Experimental and Calculated data points (ppm)	Standard Deviation from the mean($^*\sigma$)
1	128.9	129.1	-0.2	-0.1
2	125.9	123.7	2.2	0.9
3	128.4	128.2	0.2	0.1
4	118	116.5	1.5	0.6
4a	134.4	131	3.4	1.4
5a	135.5	136.9	-1.4	-0.6
6	109.8	103.4	6.4	2.7
7	148.1	146.3	1.8	0.7
8	149.8	150.1	-0.3	-0.1
9	105.9	109	-3.1	-1.3
9a	151.6	151.9	-0.3	-0.1
10a	135.1	134.3	0.8	0.3
11	166.3	169.3	-3	-1.3
15	143.3	144.1	-0.8	-0.3
16	115	116.8	-1.8	-0.7
17	127.9	131.5	-3.6	-1.5
18	125.3	125.9	-0.6	-0.3
19	127.2	125.4	1.8	0.7
20	134.8	135.4	-0.6	-0.2
20	134.8	135.4	-0.6	-0.2
21	39.5	36.5	3	1.3

Table S3. Absolute Error and the standard deviation of the error from the mean between the calculated (Structure W) and the experimental dermacozine N (**1**) ^{13}C -NMR chemical shifts

Bertalan Juhasz et al.

Nr.	Dermacozine E (8) $\delta_{^{13}\text{C}}$	Dermacozine F (9) $\delta_{^{13}\text{C}}$	Dermacozine G (10) $\delta_{^{13}\text{C}}$	Dermacozine O (2) $\delta_{^{13}\text{C}}$
1	131.7	131.9	131.8	129.6
2	127.1	127.2	127.3	126.6
3	130.7	130.9	130.9	131.3
4	119.6	119.5	119.7	120.3
4a	133.7	133.8	133.6	134.0
5a	139.0	141.9	141.7	139.5
6	99.8	95.2	95.4	100.4
7	139.6	142.7	142.5	139.6
8	133.8	134.0	133.7	134.5
9	130.2	130.4	129.9	129.7
9a	150.2	150.4	150.3	150.6
10a	135.2	135.4	135.4	135.3
11	166.2	166.4	166.3	167.2
16	121.7	119.7	119.8	122.6
17	134.2	134.5	124.3	134.1
18	131.2	131.4	132.3	131.3
19	128.1	128.3	115.2	128.2
20	127.7	127.9	158.3	127.9
21	128.1	128.3	115.2	128.2
22	131.2	131.4	132.3	131.3
23	45.9	46.0	46.3	45.9

Table S4. Experimental values of ^{13}C -NMR δ chemical shifts of dermacozines E (**8**), F (**9**), G (**9**) and O (**2**) for multiple regression and t-test

Bertalan Juhasz et al.

SUMMARY OUTPUT						
Regression Statistics						
Multiple R	0.999602					
R Square	0.999205					
Adjusted R Square	0.999064					
Standard Error	0.687836					
Observations	21					
ANOVA						
	df	SS	MS	F	Significance F	
Regression	3	10105.71	3368.569	7119.931	1.55E-26	
Residual	17	8.043009	0.473118			
Total	20	10113.75				
	Coefficients	Standard Err	t Stat	P-value	Lower 95%	Upper 95%
Intercept	-0.44071	0.939796	-0.46895	0.645066	-2.42351	1.542083
Dermacozine E (8) δ 13C	1.107188	0.113396	9.763937	2.19E-08	0.867944	1.346432
Dermacozine F (9) δ 13C	-0.1067	0.11218	-0.95118	0.354841	-0.34338	0.129976
Dermacozine G (10) δ 13C	0.00425	0.018576	0.22881	0.821746	-0.03494	0.043442
					-0.03494	0.043442
						0.043442

Hypotheses:

H₀:(null hypothesis) = the structure of dermacozine E (8) and/or dermacozine F (9) and/or dermacozine G (10) are not showing significant similarity to dermacozine O (2) (δ_C values of dermacozine E and/or dermacozine F and/or dermacozine G are independent on the corresponding δ_C values of dermacozine O).

H_a:(alternative hypothesis) = the structure of dermacozine E (8) and/or dermacozine F (9) and/or dermacozine G (10) are showing significant similarity to dermacozine O (2) (δ_C values of dermacozine E and/or dermacozine F and/or dermacozine G are dependent on the corresponding δ_C values Dermacozine O).

Bertalan Juhasz et al.

Hypothesis testing:

df (degrees of freedom) = n(number of δ_c compared)-p(number of dependent variables)-1 = 17

$\alpha = .05$

CI = 95%

$t_{\alpha/2}$ rejection region (RR) (two tailed t-test table value) = $t_{\alpha/2} \leq -2.11$ and $+2.11 \leq t_{\alpha/2}$

$t_{\alpha/2}$ values calculated, multiple regression algorithm:

$t_{\alpha/2}$ calculated value for the δ_c values in ppm of dermacozine E (8) = + 9.76;

$t_{\alpha/2}$ calculated value for the δ_c values in ppm of dermacozine F (9) = - 0.95;

$t_{\alpha/2}$ calculated value for the δ_c values in ppm of dermacozine G (10) = + 0.23;

As for dermacozine F (9) and dermacozine G (10), (calculated) $t_{\alpha/2}$ is between -2.11 and +2.11(two tailed t-test table value for $\alpha = .05$; $df = 17$), which is essentially means that $-t_{\alpha/2}$ (t-test table value) $< t_{\alpha/2}$ dermacozine F (9) (calculated) $< +t_{\alpha/2}$ (t-test table value) and $-t_{\alpha/2}$ (t-test table value) $< t_{\alpha/2}$ dermacozine G (10) (calculated) $< +t_{\alpha/2}$ (t-test table value). (Calculated $t_{\alpha/2}$ values for both molecules are not within the RR region of the t-test distribution). Therefore, we cannot reject the null hypothesis for dermacozine F (9) and dermacozine G (10). As a consequence, the δ_c values of these compounds are independent on the δ_c values of the structure of dermacozine O (2). However, when we were investigating $t_{\alpha/2}$ of dermacozine E (8) (calculated) – where there is only one substituent difference, an -NH₂ difference at position C-11 of which can change carbon shifts compared to corresponding carbon shifts in dermacozine O (2), we can see that + 9.76 $t_{\alpha/2}$ (calculated $t_{\alpha/2}$ dermacozine E) $>>$ + 2.11 $t_{\alpha/2}$ t(two tailed t-test table value. Therefore, $t_{\alpha/2}$ (calculated $t_{\alpha/2}$ dermacozine E (8)) falls into the rejection

Bertalan Juhasz et al.

region (**RR**) of the t-distribution, and as a consequence, we can reject the null hypothesis for dermacozine E (**8**) and we can accept the alternative hypothesis.

Conclusion of hypothesis testing:

The δ_C values of dermacozine O (**2**) significantly dependent on dermacozine E (**8**). Therefore, we can conclude at 95% Confidence Level that the structure of dermacozine E (**8**) is the most similar structure to dermeacozine O (**2**) among the structures of dermacozine E (**8**), F (**9**) and G (**10**), based on their corresponding δ_C values investigated with multiple regression and a two-tailed t-test.

Figure S43. Multiple regression analysis between the experimental ^{13}C -NMR δ values of dermacozines E (**8**), F (**9**), G (**9**) as independent variables and those of dermacozine O (**2**) as dependent variables

Bertalan Juhasz et al.

RESIDUAL OUTPUT		
Observation	<i>Predicted</i> <i>Dermacozone O (2)</i> $\delta^{13}\text{C}$	<i>Residuals</i>
1	131.9	-2.3
2	127.3	-0.7
3	130.9	0.4
4	119.7	0.6
5	133.9	0.1
6	138.9	0.6
7	100.3	0.1
8	139.5	0.1
9	134.0	0.5
10	130.4	-0.7
11	150.4	0.2
12	135.4	-0.1
13	166.5	0.7
14	122.0	0.6
15	134.3	-0.2
16	131.4	-0.1
17	128.2	0.0
18	128.0	-0.1
19	128.2	0.0
20	131.4	-0.1
21	45.7	0.2

Table S5. Residuals between the observed and predicted values of ^{13}C -NMR δ of dermacozines E (8), F (9), G (9) as independent variables and those of dermacozine O (2) as dependent variables

Atom Number	Experimental $\delta^{13}\text{C}$ values of Dermacozine P	ACD Labs Calculated (Neural Network Algorithm) $\delta^{13}\text{C}$ values of Dermacozine P
1	131.5	127.8
2	134.9	135.7
3	132.4	130.3
4	132.6	127.7
4a	142.4	143.6
5a	140.7	142.6
7	135.1	131.2
9	131.3	131.0
10a	142.4	140.5
11	165.5	167.3
13	166.6	164.8
15	194.4	192.1
16	136.3	139.4
17	130.0	129.9
18	128.7	128.4
19	133.5	132.2
20	128.7	128.4

Table S6. Comparison between experimental and the ACD Labs calculated ^{13}C -NMR δ chemical shift values of dermacozines P (3) (Neural Network Algorithm, DMSO- d_6)

Bertalan Juhasz et al.

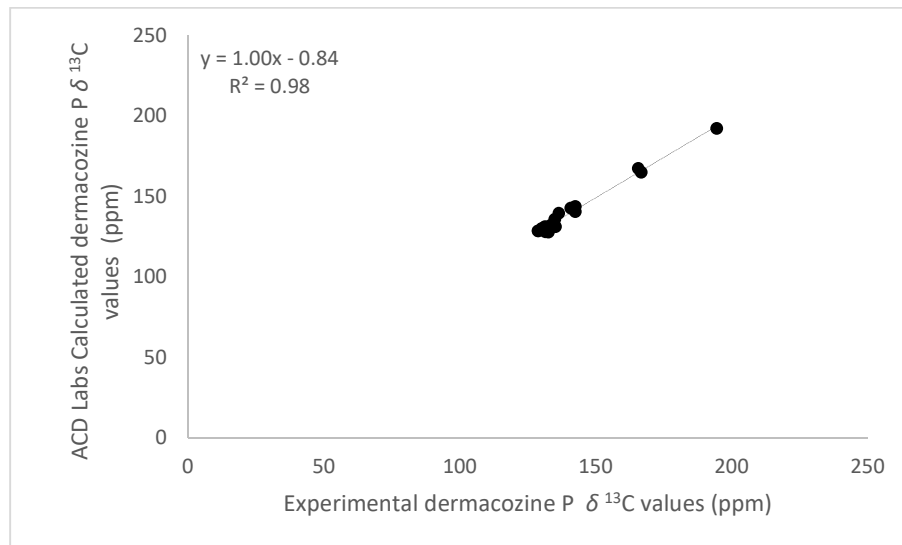


Figure S44. Linear regression graphics between the experimental ^{13}C -NMR δ chemical shifts of dermacozine P (**3**) and the ACD Labs calculated ^{13}C -NMR δ values (Neural Network Algorithm, DMSO-*d*₆)

Bertalan Juhasz et al.

Atom Number	Experimental $\delta^{13}\text{C}$ values of Dermacozone P	ACD Labs Calculated (Neural Network Algorithm) $\delta^{13}\text{C}$ values of Dermacozone P	Absolute Error (ppm)	Standard Deviation from the mean($^*\sigma$)
1	131.5	127.8	3.7	1.7
2	134.9	135.7	-0.8	-0.4
3	132.4	130.3	2.1	1.0
4	132.6	127.7	4.9	2.2
4a	142.4	143.6	-1.2	-0.5
5a	140.7	142.6	-1.9	-0.9
7	131.3	131.2	0.1	0.0
9	135.1	131	4.1	1.9
10a	142.4	140.5	1.9	0.9
11	165.5	167.3	-1.8	-0.8
13	166.6	164.8	1.8	0.8
15	194.4	192.1	2.3	1.0
16	136.3	139.4	-3.1	-1.4
17	130	129.9	0.1	0.0
18	128.7	128.4	0.3	0.1
19	133.5	132.2	1.3	0.6
20	128.7	128.4	0.3	0.1

Table S7. Absolute Error and the standard deviation of the error from the mean between the calculated and the experimental dermacozine P (**3**) ^{13}C -NMR chemical shifts

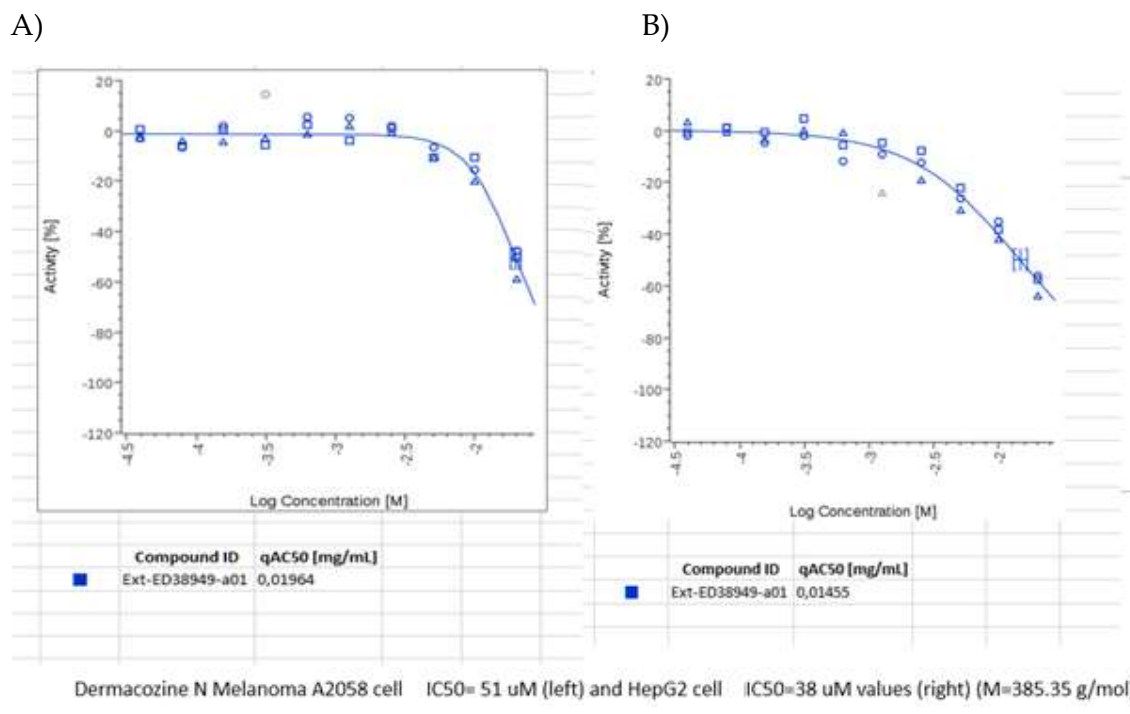
Bertalan Juhasz et al.


Figure S45. Evaluation of the cytotoxic activity of dermacozine N (**1**) against human A) Melanoma (A2058) and B) Hepatocellular carcinoma (HepG2) cell lines (IC₅₀ graphs)

Bertalan Juhasz et al.

No.	<i>Dermacozone N (1)</i>				
	δ_c , mult	δ_h , mult (<i>J</i> in Hz)	HMBC	COSY	NOESY
1	128.9, C		3		
2	125.9, CH	7.88 (dd, 7.6, 1.3)	4	3	
3	128.4, CH	7.47 (td, 8.3, 7.6)		4, 2	
4	118.0, CH	7.55 (dd, 8.3, 1.3)	2	3	
4a	134.4, C		3, 23		
5a	135.5, C		9, 23		
6	109.8, C		14		
7	148.1, C		9		
8	149.8, C		9		
9	105.9, CH	6.79, s			12.A, 12.B
9a	151.6, C		9		
10a	135.1, C		2, 4		
11	166.3, C		2		
12		A 7.70, brs B 9.31, brs		12.B 12.A	12.B 12.A
13	168.3, C [†]				
14		A 7.65, brs B 7.98, brs		14.B 14.A	14.B 14.A
15	143.3, C		16, 17, 19		
16	115.0, CH	7.12 (dd, 7.6, 1.5)	18	17	
17	127.9, CH	7.19 (ddd, 7.6, 7.4, 1.6)	19	16, 18	
18	125.3, CH	7.15 (ddd, 7.6, 7.4, 1.5)	16	17, 19	
19	127.2, CH	7.30 (dd, 7.6, 1.6)	17	19	
20	134.8, C		16, 18		
21					
22					
23	39.5, CH ₃	3.68, s			4

Table S8. Experimental NMR spectroscopic data for dermacozine N (1) with HMBC, COSY and NOESY correlations (800 MHz, DMSO-*d*₆)

[†]: Calculated with ACD Labs Software, Neural Network Algorithm, DMSO-*d*₆ (Chemical shift is not observed)

Bertalan Juhasz et al.

No.	<i>Dermacozone O (2)</i>			
	δ_{C} , mult	δ_{H} , mult (J in Hz)	HMBC	COSY
1	129.6, C		3	
2	126.6, CH	7.87 (dd, 7.5, 1.1)	4	3
3	131.3, CH	7.78 (td, 8.5, 7.5)		2, 4
4	120.3, CH	7.97 (dd, 8.5, 1.1)	2	3
4a	134.0, C		3, 23	
5a	139.5, C		9, 23	
6	100.4, C		8, 14	
7	139.6, C		8, 9	
8	134.5, CH	7.21 (d, 9.7)		9
9	129.7, CH	7.24 (d, 9.7)		8
9a	150.6, C		8, 9	
10a	135.3, C		2, 4	
11	167.2, C		2	
12		COOH, not observed		
13	163.6, C [†]			
14		11.27, bs		
15	163.1, C [†]			
16	122.6, C		8, 14, 18, 22	
17	134.1, C		19, 21	
18	131.3, CH	7.30 (dd, 7.4, 1.3)	19, 20	19/21
19	128.2, CH	7.47 (td, 7.4, 1.3)	18, 21	18/22, 20
20	127.9, CH	7.41 (td, 7.4, 1.3)	18, 21	19, 21
21	128.2, CH	7.47 (td, 7.4, 1.3)	19, 22	18/22, 20
22	131.3, CH	7.30 (dd, 7.4, 1.3)	20, 21	21/19
23	45.9, CH ₃	3.67, s		

Table S9. Experimental NMR spectroscopic data for dermacozine O (2) with HMBC and COSY correlations (800 MHz, DMSO-*d*₆)

[†]: Calculated with ACD Labs Software, Neural Network Algorithm, DMSO-*d*₆ (Chemical shift is not observed)

Bertalan Juhasz et al.

No.	<i>Dermacozone P (3)</i>				
	δ_{C} , mult	δ_{H} , mult (<i>J</i> in Hz)	HMBC	COSY	Selective-NOESY, irrad. at 8.03 ppm
1	131.5, C		3		
2	134.9, CH	8.74 (dd, 7.0, 1.3)	4	3	
3	132.4, CH	8.21 (td, 7.0, 8.6)		4, 2	
4	132.6, CH	8.55 (dd, 8.6, 1.3)	2	3	
4a	142.4, C		3		
5a	140.7, C		7, 9		
6	129.8, C [†]				
7	131.3, CH	8.65 (d, 1.9)	9		
8	135.6, C [†]				
9	135.1, CH	8.95 (d, 1.9)	7		
9a	144.0, C [†]				
10a	141.2, C		2, 4		
11	165.5, C				
12		COOH, not observed			
13	166.6, C		7		
14		A 8.03, brs B 9.47, brs			17/21
15	194.4, C		9, 17, 21		
16	136.3, C		17, 18, 20, 21		
17	130.0, CH	7.95 (dd, 7.6, 1.3)	18, 19	18/20	
18	128.7, CH	7.66 (td, 7.6, 1.3)	20	19, 17/21	
19	133.5, CH	7.78 (td, 7.6, 1.3)	17, 21	18/20	
20	128.7, CH	7.66 (td, 7.6, 1.3)	18	19, 17/21	
21	130.0, CH	7.95 (dd, 7.6, 1.3)	17, 19	18/20	
22	-	-	-	-	-
23	-	-	-	-	-

Table S10. Experimental NMR spectroscopic data for dermacozine P (3) with HMBC and COSY correlations (600 MHz, DMSO-*d*₆)

[†]: Calculated with ACD Labs Software, Neural Network Algorithm, DMSO-*d*₆ (Chemical shift is not observed)

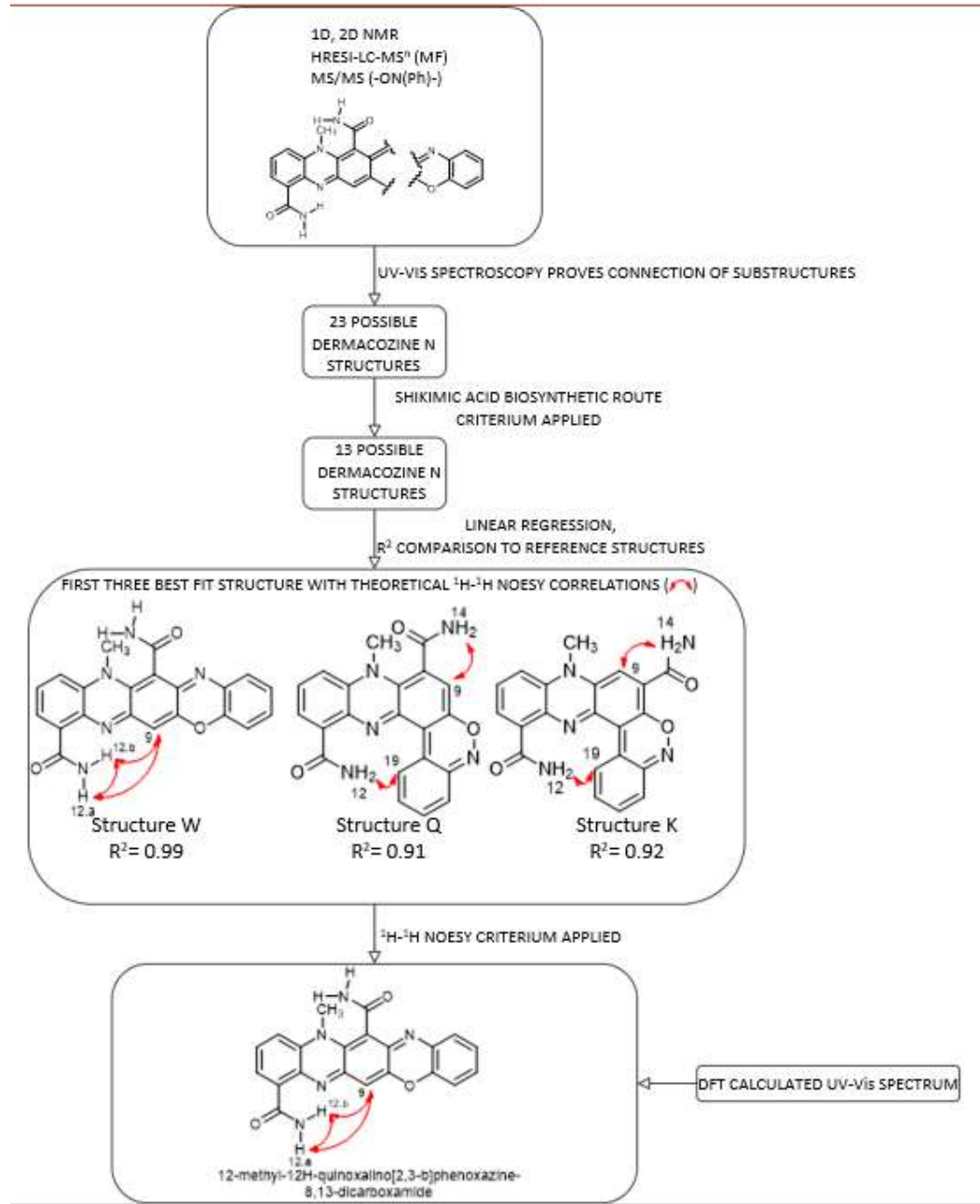
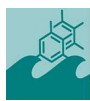


Figure S46. Workflow of dermacozine N (1) structure determination



Bertalan Juhasz et al.

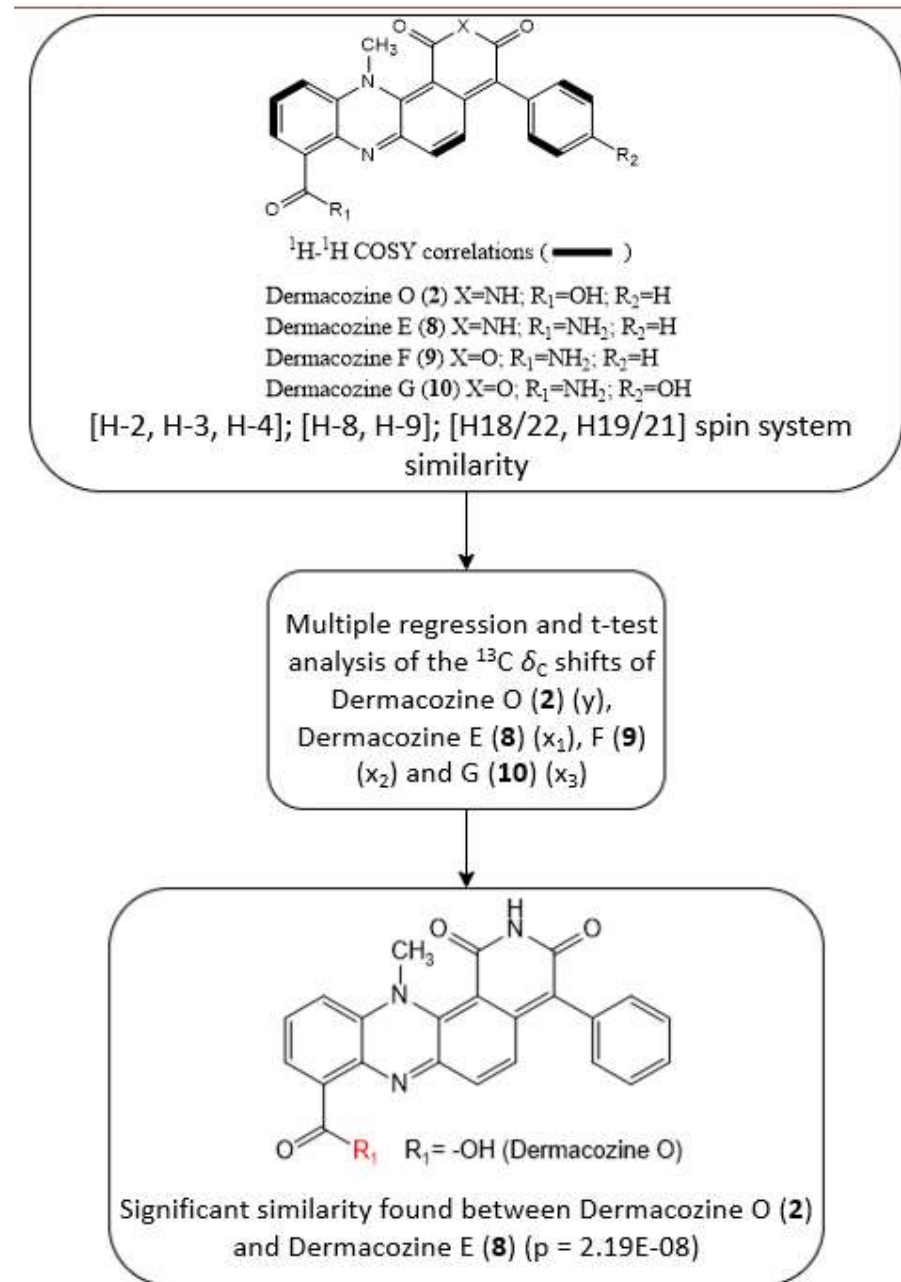


Figure S47. Workflow of dermacozine O (**2**) structure determination.

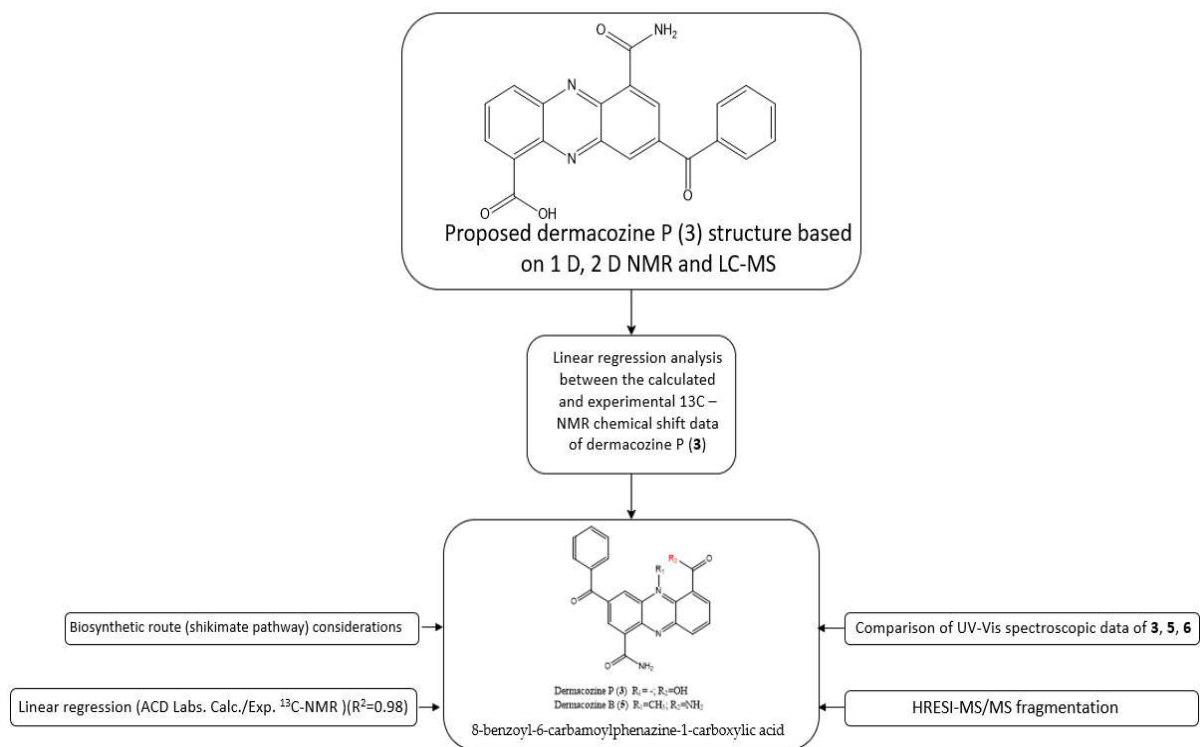
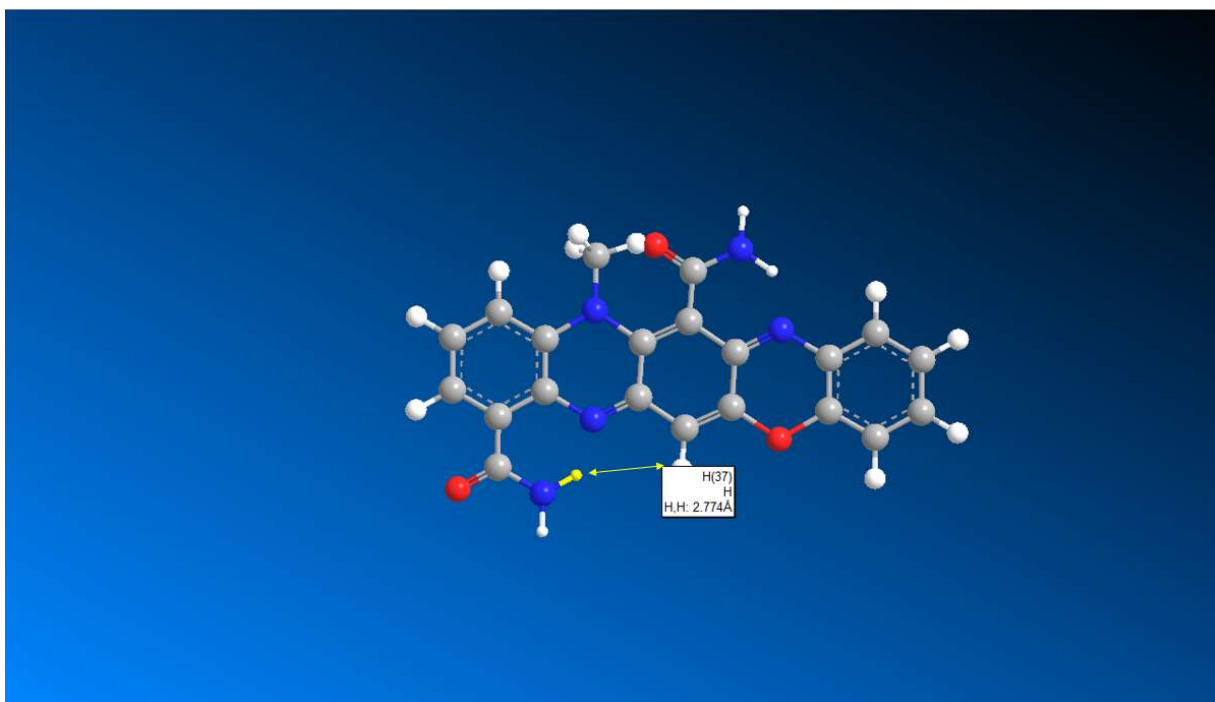
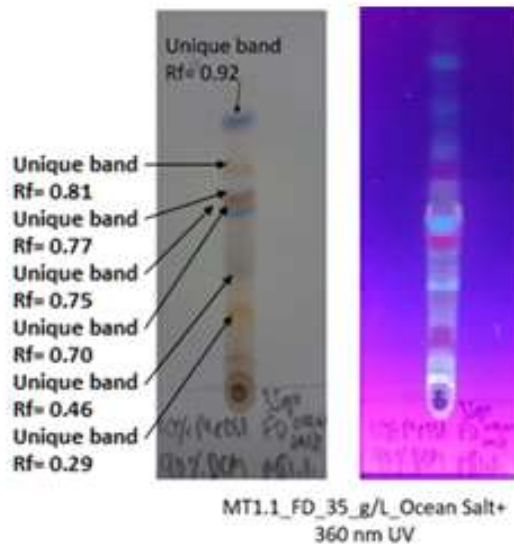
Bertalan Juhasz et al.


Figure S48. Workflow of dermacozine P (3) structure determination

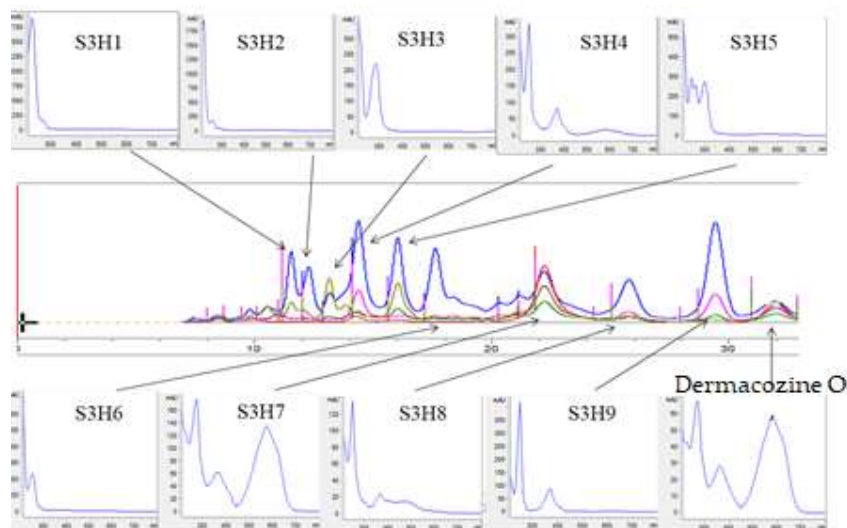
Bertalan Juhasz et al.



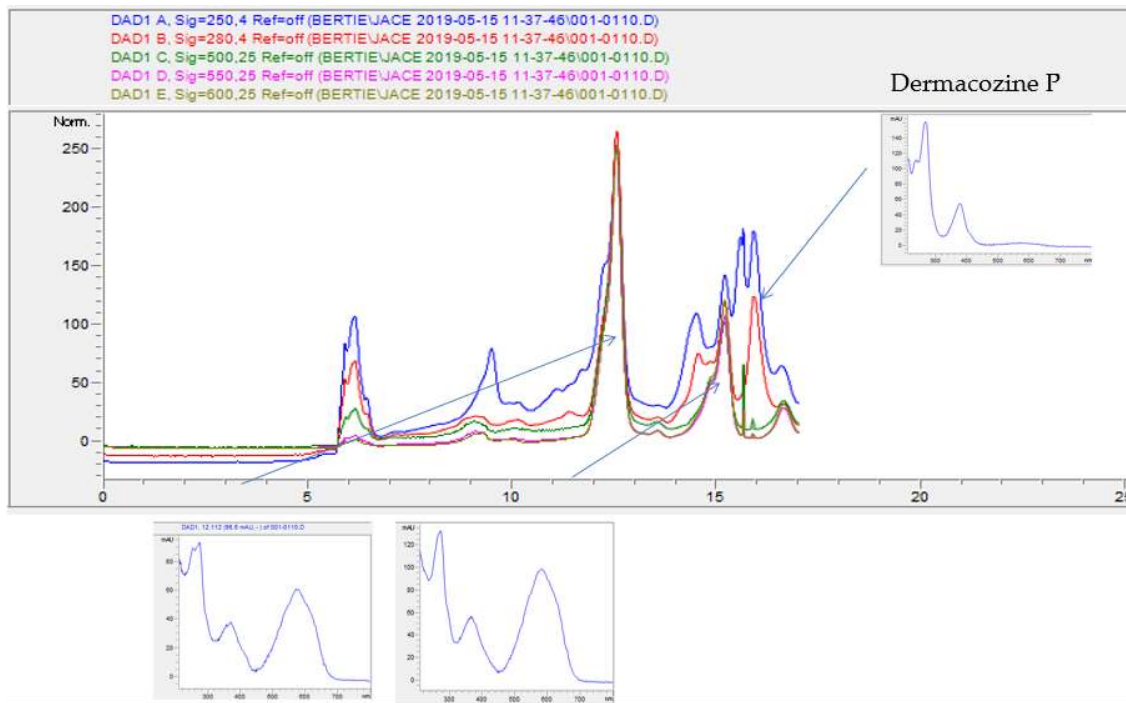
Theme S1. Dermacozine N (1) H-9 and NH₂-12 distance (Modelled with Chemdraw, Chem 3D)



Theme S2. TLC plate of the initial FD fraction following Kupchan liquid-liquid partitioning, showing the colorful bands where the dermacozines were isolated from (left) and the same TLC plate under UV 360 nm light (right)



Theme S3. HPLC chromatogram for the isolation of dermacozine O (2)

Bertalan Juhasz et al.


Theme S4. HPLC chromatogram for the isolation of dermacozine P (3)